The Journal of Experimental Biology 200, 1383–1402 (1997)
Printed in Great Britain © The Company of Biologists Limited 1997
JEB0802

NEURAL MECHANISMS OF ADAPTIVE GAIN CONTROL IN A JOINT CONTROL LOOP: MUSCLE FORCE AND MOTONEURONAL ACTIVITY

ROLF KITTMANN*

Institut für Zoologie, Albertstraße 21a, Albert-Ludwigs-Universität Freiburg, D-79104 Freiburg, Germany
and *Fachbereich Biologie, Universität Kaiserslautern, Postfach 3049, D-67663 Kaiserslautern, Germany*

Accepted 12 February 1997

Summary

An adaptive gain control system of a proprioceptive feedback system, the femur–tibia control loop, is investigated. It enables the joint control loop to work with a high gain but it prevents instability oscillations. In the inactive stick insect, the realisation of specific changes in gain is described for tibial torque, for extensor tibiae muscle force and for motoneuronal activity. In open-loop experiments, sinusoidal stimuli are applied to the femoral chordotonal organ (fCO). Changes in gain that depend on fCO stimulus parameters (such as amplitude, frequency and repetition rate), are investigated. Furthermore, spontaneous and touch-induced changes in gain that resemble the behavioural state of the animal are described.

Changes in gain in motoneurones are always realised as changes in the amplitude of modulation of their discharge frequency. Nevertheless, depending on the stimulus situation, two different mechanisms underlie gain changes in motoneurones. (i) Changes in gain can be based on changes in the strength of the sensorimotor pathways that transmit stimulus-modulated information from the fCO to the motoneurones. (ii) Changes in gain can be based on changes in the mean activity of a motoneurone by means of its spike threshold: when, during the modulation, the discharge of a motoneurone is inhibited for part of the stimulus cycle, then a change in mean activity subsequently causes a change in modulation amplitude and gain.

A new neuronal mechanism is described that helps to compensate the low-pass filter characteristics of the muscles by an increased activation, especially by a sharper distribution of spikes in the stimulus cycle at high fCO stimulus frequencies.

Key words: adaptive gain control, proprioceptive feedback, joint control loop, tactile stimulus, motoneurone, reflex modulation, neuronal gain mechanisms, stick insect, *Carausius morosus*.

Introduction

The adaptive properties of the nervous system enable an animal to show flexible reactions in response to a stimulus, depending on the situation. The control of the gain of reflexes, an important mechanism underlying adaptive behaviour, has been investigated in many systems from the behavioural to the neuronal level (for reviews, see Prochazka, 1989; Burrows, 1992, 1994; Pearson, 1993; Morton and Chiel, 1994).

Adaptive behaviour in many cases also requires a modification of the properties of biological feedback systems. The control of feedback gain is the main mechanism by which this occurs: most of the parameters that influence the characteristics of a feedback system, such as its latency and its dynamics, are determined and limited by constraints arising from the morphology and the physiology of its components. In contrast, the gain, the ratio between the amplitude of the response and that of the stimulus, which is responsible for the efficiency, speed, accuracy and stability of the feedback system, can be varied by several neuronal mechanisms. In vertebrates and invertebrates, adaptive gain control is a common property of feedback systems and has been demonstrated in various systems (DiCaprio and Clarac, 1981; Field and Burrows, 1982; Cruse and Schmitz, 1983; Burrows and Laurent, 1989; El Manira *et al.* 1990, 1991; Kirschfeld, 1991, 1992; Skorupski *et al.* 1994; for reviews, see Prochazka, 1989; Pearson, 1993; Burrows, 1994). The gain value can depend on several factors, including the stimulus parameters, the task performed and the behavioural state of the animal. In the field of clinical diagnostics, increased importance has recently been given to measurements of the gain of feedback systems (Waterston *et al.* 1992; Davis and O'Leary, 1993; Bloem *et al.* 1995).

Proprioceptive feedback systems in insects that control the posture and movements of the legs have proved to be excellent models with which to analyse the neuronal basis of information processing (Wendler, 1964; Bässler, 1972*a*,*b*; Burrows, 1974; Cruse and Storrer, 1977; Cruse and Schmitz, 1983; Zill, 1985; Schmitz, 1985, 1986, 1993; Burrows *et al.* 1988). The behavioural function of the femur–tibia feedback system in

*e-mail: kittmann@sun2.ruf.uni-freiburg.de.

stick insects and locusts is especially well understood, and the complexity of the neuronal circuitry is low compared with that of vertebrates. Thus, it has been possible to identify many of the neurones involved, to uncover the coarse structure of the circuitry and to understand the main principles of information processing in this system (locusts: Burrows, 1974, 1980, 1987; Field and Burrows, 1982; stick insects: Büschges, 1990; Kittmann and Schmitz, 1992; Driesang and Büschges, 1993, 1996; Büschges and Wolf, 1995; for reviews, see Bässler, 1983*a*, 1993; Burrows, 1994). Nevertheless, there is a gap in our understanding between the detailed descriptions of gain control in the whole system and its functions in behaviour (Kittmann, 1984, 1991; Bässler and Nothof, 1994) on the one hand, and the analysis of the neuronal mechanisms that possibly form the neuronal basis of gain control on the other (Field and Burrows, 1982; Laurent and Burrows, 1989; Ramirez *et al.* 1993; Büschges *et al.* 1993; Burrows and Matheson, 1994; Jellema and Heitler, 1996; Büschges and Wolf, 1996). The functional significance of neuronal mechanisms in gain control remains to be tested under conditions in which behaviourally relevant changes in gain occur or can be induced.

Therefore, in the present study, the neuronal realisation of gain control is investigated for the femur–tibia control loop of the stick insect, for which adaptive changes in gain and their function in behaviour have been demonstrated previously (Kittmann, 1991; Bässler and Nothof, 1994). This feedback system is highly adaptive as its characteristics depend strongly on the behavioural situation of the animal (for reviews, see Bässler, 1983*a*, 1993). In the inactive animal, different types of inputs to the gain control system, which either increase or decrease the gain depending on the requirements of the situation of the animal, have been characterised (Kittmann, 1991). Even in the inactive animal, changes in gain (calculated from the movement amplitude of the tibia) of more than 50-fold may occur naturally or can be induced. Following a disturbance of the animal, e.g. by a tactile stimulus, the gain of the system is high and this results in a strong resistance to imposed passive movements of the tibia. Thus, the posture is stabilised and produces 'twig mimesis', a camouflage behaviour of stick insects. A 'self-calibrating gain control system' enables the animal to optimise the gain to a critical upper value, high enough for the most efficient feedback response but limited to a value that prevents instability. The function of this gain control system is based on the following properties: (i) an increase in gain produced by perturbing stimuli, e.g. tactile stimuli, (ii) a decrease in gain during repetitive stimulation, and (iii) a non-linear gain *versus* stimulus amplitude relationship (Kittmann, 1991). Several experiments have proved that this gain control system avoids instability in the closed-loop system (Bässler and Nothof, 1994), a common problem of many technical and biological feedback systems.

The present investigation demonstrates these properties of the gain control system for the tibial torque, the extensor tibiae muscle force and the motoneuronal activity of the extensor muscle. It revealed two independent neuronal mechanisms for the control of gain, the use of which depended on the behavioural situation: (i) changes in gain can be based on changes in the strength of sensorimotor pathways that transmit stimulus-modulated information from the femoral chordotonal organ (fCO) to the motoneurones; (ii) changes in gain can be based on changes in the mean activity of a motoneurone by means of its spike threshold. If the discharge of a motoneurone is inhibited for a part of the stimulus cycle, then a change in its mean activity subsequently causes a change in its modulation amplitude and gain.

Materials and methods

All experiments were carried out on adult female stick insects *Carausius morosus* (Brunner) obtained from the colonies at the University of Kaiserslautern and the University of Freiburg, Germany.

Preparation

For the open-loop analysis, direct mechanical stimulation of the fCO was carried out as described by Kittmann (1991). The apodeme of the fCO was cut from its insertion at the tibia and clamped into a pair of forceps that could be moved by a pen motor. Elongation and relaxation of the fCO simulated flexion and extension movements of the tibia and induced a resistance reflex by the activation of extensor or flexor tibiae motoneurones and muscles. The femur–tibia angle, the force at the tibia and the force of the extensor tibiae muscle were measured. Electrophysiological recordings from the extensor nerve (F2) were obtained using steel wires (50 μm) insulated except at the tips.

The femur–tibia (FT) angle was measured using an opto-electronic device with a resolution of less than 1 ° (for details, see Kittmann, 1991). The torque at the tibia resulting from the contraction of the two antagonistic muscles was calculated from the force measured at the tibia by an isometric strain gauge transducer (SWEMA, SG4-90, 90 mN full scale). An indirect measurement of the extensor muscle force at the tibia was possible after disconnecting the flexor muscle apodeme from the tibia (Storrer and Cruse, 1977). The true extensor muscle force was then calculated using the ratio of the tibial lever arms of the muscle and of the force transducer.

Behavioural state of the animal and stimulus program

Stick insects camouflage themselves using twig mimesis and are therefore inactive under daylight conditions. During the experiments, the animals were in this inactive behavioural state in which no spontaneous leg movements occur. Nevertheless, in the inactive animal, leg movements can be elicited as proprioceptive feedback responses. These reflex responses can be increased by arousing the inactive animal, e.g. by using tactile stimuli (Bässler, 1983*a*; Kittmann, 1991). Sine-wave stimulus trains of 20–50 sine-wave cycles with frequencies from 0.01 to 10 Hz were applied to the fCO. Stimulus amplitudes ranged from 50 to 500 μm, corresponding to tibial

movement amplitudes of 10–100 ° FT angle, adjusted to give a central position of 90 °. Stimulus trains were separated by pauses of 4 min. To dishabituate the animal and to increase the gain, a tactile stimulus was applied with a paint brush to the abdomen of the animal 10 s before each stimulus train (for details, see Kittmann, 1991).

Data recording and evaluation

Force measurements

Femoral chordotonal organ stimulus function, FT angle, muscle force and motoneuronal activity were recorded using an FM tape recorder (Racal store 4) or a DAT recorder (DTR-1801). Muscle force and stimulus function were evaluated from pen recordings (Hellige HE19) using a digitising tablet (Apple Graphics Tablet) or were fed directly into a computer interface (CED-1401) and analysed on computer. Force parameters, extreme values, amplitudes and phase shifts were evaluated for the first, fifth, tenth, fifteenth and twentieth stimulus cycle. The modulation of extensor muscle force by sinusoidal fCO stimulation is not a pure sine function. Therefore, two values of phase shift were calculated, one between the maximum fCO elongation and the maximum extensor muscle force, the other between the maximum fCO relaxation and the minimum extensor force. As both curves were similar, only the first is shown in the results.

Electrophysiological recordings

The extensor muscle is innervated by one inhibitory and two excitatory motoneurones. In extracellular recordings from the extensor nerve, the three motoneurones can easily be distinguished by the amplitude of their action potentials and by their response characteristics. The fast extensor tibiae motoneurone (FETi), with the largest spike amplitude, is only active during strong movements of the leg. The slow extensor tibiae motoneurone (SETi), which has medium-sized spikes, is spontaneously active and its activity is strongly modulated by fCO movement. The common inhibitor motoneurone (CI1), which has the smallest spikes, fires only rarely in the inactive animal (see Bässler, 1983*a*). A window discriminator transformed the extracellular recordings from the three motoneurones to three channels of digital pulses. These pulse trains were analysed using computer programs. Four variables are used to characterise the motoneuronal activity during each stimulus cycle: the mean activity (mean), the maximum activity (max), the amplitude of modulation of the discharge frequency (mod) and the mean vector length (Vl). The mean activity was calculated as the number of action potentials per stimulus cycle divided by the cycle duration. The maximum activity was calculated from the spike distribution using circular statistics (see below). The amplitude of modulation gives the difference between the mean activity and the maximum activity. The mean vector length gives a measure of the distribution of spikes within the stimulus cycle (see below).

Circular statistics

The fCO stimulus frequency covered a 1000-fold range, from 0.01 to 10 Hz. Depending on the duration of the stimulus cycle and the spontaneous activity of the SETi neurone, the number of action potentials per stimulus cycle ranged from fewer than 10 (at 10 Hz fCO frequency) to more than 2000 (at 0.01 Hz). This made it difficult (and would have introduced artificial variation) to determine the maxima and minima of the discharge frequency by conventional methods, e.g. from the instantaneous frequency or from peri-stimulus spike histograms. Therefore, circular statistics were used to describe the modulation of motoneuronal discharge as a spike distribution over the stimulus cycle and to calculate the maximum SETi discharge frequency (Batschelet, 1981; Heukamp, 1983; Kittmann and Schmitz, 1992). Compared with conventional methods, the neuronal discharge parameters calculated using circular statistics have two main advantages: they can be calculated for the whole stimulus frequency range using a single method and they are based on all spikes occurring in the stimulus cycle. Therefore, they are more reproducible, show smaller statistical variation and thus allow the description of small continuous changes in the motoneuronal discharge and gain (for examples, see Figs 7, 9, 10).

Each spike is taken as a unit vector with a phase angle according to its occurrence in the stimulus cycle. A resultant vector is calculated by the vector addition of all spike vectors within one stimulus cycle, with the total length divided by the number of spikes. This mean vector length (Vl), which has a value between 0 and 1, is a measure of the distribution of the spikes within a stimulus cycle. A value of 0 means that the spikes are evenly distributed over the stimulus period and that there is no sinusoidal modulation of discharge. A value near 1 characterises a discharge pattern in which all spikes occur within a small range of phase angles over the stimulus cycle. A value of 0.5 means that the amplitude of sinusoidal modulation of spike frequency is equal to the mean activity, and therefore gives a maximum frequency of twice the mean frequency and a minimum frequency near zero. The phase angle of the mean vector (mean vector angle) describes the phase relationship between the stimulus and the response, especially between maximum fCO elongation and maximum SETi discharge.

For a sinusoidally modulated spike frequency, the maximum frequency (max) and the amplitude of modulation (mod) can be calculated from the two independent parameters measured: the mean activity (mean) and the mean vector length (Vl) where:

$$\text{mod} = 2 \times \text{mean} \times \text{Vl}$$

and

$$\text{max} = \text{mean} + \text{mod}.$$

Values of Vl below 0.5 therefore characterise a discharge pattern in which the mean activity exceeds the modulation: the spontaneous activity of the neurone is modulated and the spikes occur during the whole stimulus cycle (e.g. see Fig. 4A,C). Values of Vl between 0.5 and 0.8 characterise a discharge with a strong modulation of spontaneous activity: modulation exceeds the mean activity. Therefore, for part of

the stimulus cycle (<180 °), the motoneuronal discharge is completely inhibited and the activity of the neurone, plotted as an instantaneous frequency plot (e.g. see Figs 1, 2) or as a peri-stimulus time histogram (e.g. see Figs 4B, 13Cii), looks like a sine wave clipped at the 0 Hz line, since the motoneurone cannot produce negative frequency values. Values of Vl higher than 0.8 characterise the spike distributions of neurones that are not spontaneously active (e.g. FETi). The modulation of their input by the fCO stimulus causes a discharge limited to phase angles of less than 180 ° of the stimulus cycle.

The amplitude of modulation and the maximum frequency of a sinusoidally modulated spike activity calculated using circular statistics are correct for mean vector lengths between 0 and 0.5 (see below). For mean vector lengths between 0.5 and 1, the amplitude of modulation exceeds the mean activity. In this case, mean activity and mean vector length values calculated using circular statistics, and the amplitude of modulation and the maximum frequency calculated from these values, differ from the values of these parameters characterising the sine wave underlying the sinusoidally modulated spike frequency. Therefore, for mean vector lengths greater than 0.5, the values of amplitude of modulation and maximum frequency determined from the experimental data were corrected using results from computer-simulated spike distributions (see below).

Computer simulation

To test the extent to which motoneuronal spike frequencies were sinusoidally modulated, SETi discharge frequencies recorded during sinusoidal fCO stimulation were compared with sinusoidally modulated spike frequencies from a computer simulation. For strong modulations of SETi discharge in particular, computer simulations were necessary to reveal the parameters of the sine-wave function underlying the instantaneous frequency and to draw conclusions concerning the inputs of the neurone (see below and Discussion).

Sinusoidally modulated instantaneous spike frequencies with a preset mean frequency ($mean_s$, where s stands for simulated) and amplitude of modulation (mod_s) were created using a computer program. The intended instantaneous frequency ($F_{s(t)}$) was defined as a sine function of time (t):

$$F_{s(t)} = mean_s + [mod_s \times \sin(2\pi t/T)],$$

where T is the sine-wave period.

The instantaneous frequency of a certain spike ($F_{s(spike)}$) within the stimulus cycle depends on its time delay (d) with regard to the previous spike:

$$F_{s(spike)} = 1/d.$$

The first spike was positioned somewhere at the beginning of the sine-wave function. The position of the following spike was defined by the time when both frequencies, the intended instantaneous frequency ($F_{s(t)}$) and the instantaneous frequency of that spike ($F_{s(spike)}$, defined by its delay to the previous spike), were equal. This point was determined by an iteration algorithm. All following spikes were successively positioned by this method. As the result depends to some extend on the position of the first spike in the sine-wave cycle, several successive sine-wave periods were simulated until a stable spike distribution was obtained. The parameters, mean frequency ($mean_s$) and amplitude of modulation (mod_s), used as input for the simulated sinusoidal spike frequencies were compared with the values of these parameters revealed by circular statistics (mean, mod) from these spike distributions.

For mean vector lengths up to 0.5, the results demonstrate that the values used for the simulation and the values obtained using circular statistics were almost identical. For vector lengths greater than 0.5, comparison of the values used as input to the simulation with the results using circular statistics showed systematic differences. The mean activity values from circular statistics (mean) always exceeded the corresponding value ($mean_s$) used as input for the simulation spike frequency. The modulation value (mod) derived from circular statistics was smaller than the value used as input for the simulation (mod_s). The maximum frequency from circular statistics (max = mean + mod) was always slightly smaller than the value ($max_s = mean_s + mod_s$) calculated from the inputs to the simulation. The magnitude of these effects increased with increasing mean vector length.

The comparison of mean activity and amplitude of modulation values in simulated spike distributions with the experimental data allowed determination of correct values for the mean activity and amplitude of modulation values characterising the sinusoidally modulated discharge frequency, even for spike distributions clipped by the motoneurone's spike threshold. With these corrections, appropriate conclusions could be drawn concerning the synaptic input to motoneurones that determine the parameters of their discharge *via* changes in the mean value or the modulation of the membrane potential (see Discussion).

Statistics

The Wilcoxon–Mann–Whitney U-test was used to compare the muscle force and SETi discharge variables at different stimulus frequencies (e.g. see Figs 3, 6) or stimulus amplitudes (e.g. see Fig. 5). $P<0.05$ was taken as the limit of significance.

During repetitive fCO stimulation within a stimulus train, most of the parameters that characterised the response changed continuously but showed small variations (e.g. see Figs 1, 2, 7). The significance of these changes for the muscle force and SETi discharge variables during repetitive stimulation within stimulus trains was tested using paired t-tests. Unless noted otherwise, the values from the first and twentieth stimulus cycle were compared. The standard deviation in these cases (e.g. see Figs 3, 6A,B) mainly reflects the variation between the absolute values of these variables among different animals and cannot be used to estimate the significance of the changes in these variables during repetitive stimulation. For clarity, standard deviation is only indicated for the first and the twentieth (occasionally the fiftieth) stimulus cycle in these

cases. Standard deviation values for the other cycles were similar since the data are derived from the same stimulus trains.

Results

Changes in gain in the femur–tibia control loop have been described in detail for the open-loop system, where the resistance movement of the tibia was measured as the amplitude of the FT angle (Kittmann, 1991). These movements are caused by activation of two antagonistic muscles, the flexor and the extensor tibiae. To understand the changes in gain for the torque at the tibia, the force generated by the extensor tibiae muscle and the underlying motoneuronal activity, in the present study, stimulus programs were applied to the fCO that are known to induce changes in the gain of the whole system.

Force measurements

Both the torque at the tibia (Fig. 1) and the force produced by the extensor muscle (Fig. 2) are modulated by the fCO stimulus, and changes in gain could be measured as changes in the amplitude. The main properties of the gain control system described previously for tibial movement (Kittmann, 1991) were also observed for these output functions. There was a decrease in gain during repetitive sinusoidal stimulation, an important property of the gain control system that preserves the stability of the FT control loop, both for tibial torque (Fig. 1) and for extensor muscle force (Fig. 2). An increase in gain caused by a disturbing tactile stimulus (Fig. 2) and a spontaneous recovery of force amplitude during the stimulus pauses (results not shown) were also present for these output functions.

Quantitative measurements of the extensor muscle force variables are summarised in Fig. 3. The amplitude–frequency curves show band-pass characteristics with maximum amplitudes at fCO stimulus frequencies between 0.05 and 0.5 Hz (Fig. 3A). At low stimulus frequencies, the extensor muscle is able to relax almost fully during the stimulus phase when the flexor is excited (Fig. 2). Therefore, force minima are low (<10 mN) at these frequencies. At stimulus frequencies above 1 Hz, a strong significant decrease of extensor muscle force amplitude (Fig. 3A) and a more negative phase shift (Fig. 3B) are caused by the low-pass characteristics of the muscle. The decrease in force amplitude is caused primarily by an increase in the force minima (Fig. 3C): the stimulus cycle period is too short to allow full relaxation of the muscle. This increase in the force minima leads to co-contraction of the antagonistic muscles at higher stimulus frequencies (see Storrer and Cruse, 1977). The effects of co-contraction on the system characteristics of a similar feedback system have been described in detail by Bässler and Stein (1996). Co-contraction affects the dynamics and gain of the system. It probably also determines the centre position of the tibial movement during resistance reflexes.

The decrease in gain during repetitive sinusoidal stimulation is represented as a significant decrease in the extensor muscle force amplitude between cycle 1 and cycle 20 at all tested stimulus frequencies (Fig. 3A). Between the first and twentieth cycle, the mean extensor force amplitude was significantly reduced to between 68 % (0.01 Hz) and 39 % (2 Hz) of the initial value. For individual stimulus trains, extreme reductions in force amplitude (by 85 %) were observed within 20 stimulus cycles.

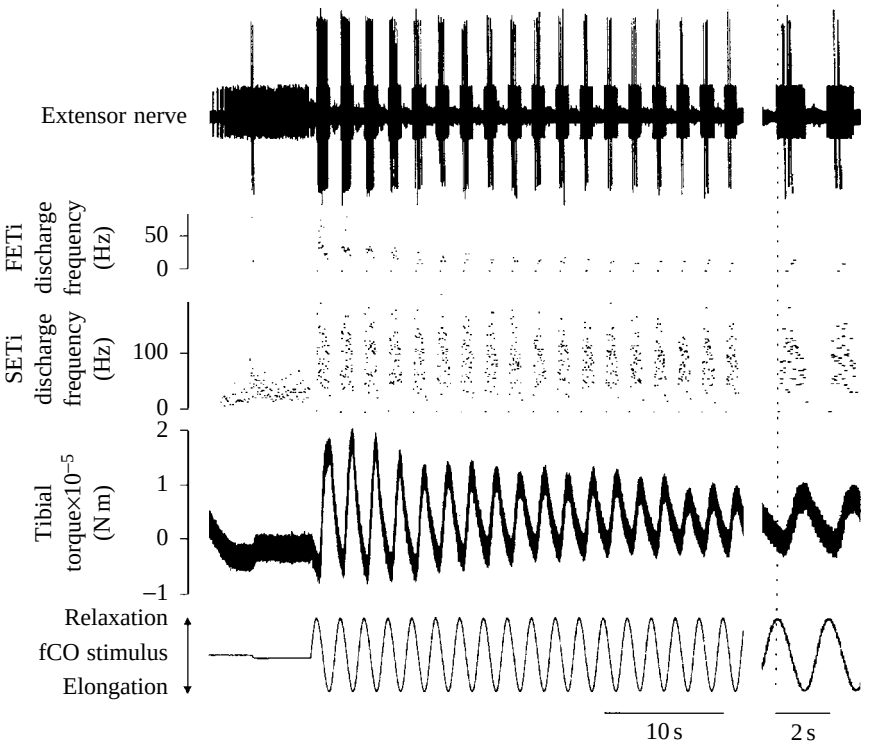

Fig. 1. Decrease in tibial torque during repetitive sinusoidal stimulation of the femoral chordotonal organ (fCO). The decrease in torque amplitude is accompanied by a decrease in FETi (large action potentials) and SETi discharge frequency. Traces show (from top to bottom): recording from the extensor nerve, the instantaneous discharge frequency of the FETi and SETi motoneurones, tibial torque, and the fCO stimulus pattern (0.5 Hz, 300 µm amplitude, scale bar 10 s). Right-hand panel gives the last two cycles on an extended time scale (scale bar 2 s) to show the phase relationship (dotted vertical line) between maximum relaxation and extensor nerve activity.

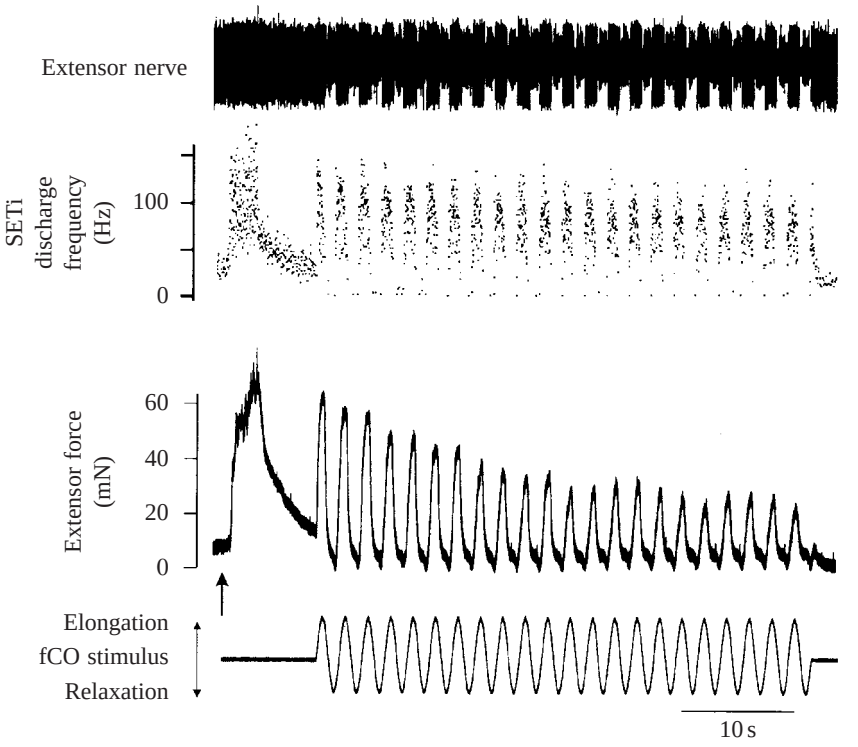

Fig. 2. Decrease in extensor muscle force and SETi discharge frequency during repetitive sinusoidal stimulation of the femoral chordotonal organ (fCO). Initial excitation of the SETi motoneurone (arrow) was caused by the tactile stimulus used to dishabituate the animal. Traces show (from top to bottom): recording from the extensor nerve, the instantaneous discharge frequency of the SETi motoneurone, the extensor muscle force and the fCO stimulus pattern (0.5 Hz, 300 μm amplitude, scale bar 10 s).

From the first to the twentieth fCO stimulus cycle, a weak, but not significant (paired *t*-test, $P>0.1$, $N\geqslant 8$), decrease in the mean phase shift between maximum fCO elongation and maximum force (Fig. 3B) and maximum fCO relaxation and minimum force (between −2 ° and −12 °, results not shown) was found for all stimulus frequencies. At a stimulus frequency of 2 Hz, an increased number of stimulus cycles (N=96) was evaluated to test the significance of this decrease. The mean phase shifts for the force maxima and minima of stimulus cycles 15–20 were significantly smaller than the values for stimulus cycles 1–5 (differences were −8 ° and −12 °, respectively, paired *t*-test, $P<0.05$).

The reduction in force amplitude during repetitive sinusoidal stimulation was found to be due mainly to a significant reduction in the force maxima, while the force minima (which determine the degree of co-contraction of the antagonistic muscles) remained relatively constant (Fig. 3C). Spontaneous changes in gain and extensor force amplitude or those induced by tactile stimuli are also caused primarily by changes in the maximum value of the extensor force (e.g. Fig. 10).

The shape of the extensor muscle force amplitude–frequency curve changes when the gain of the system decreases, and therefore the filter characteristics of the feedback loop also change.

Motoneuronal activity

One objective of this study was to describe how changes in gain are represented at the level of motoneuronal activity. The motoneurones of the extensor tibia muscle are particularly well suited for such a quantitative description since this muscle is innervated by only two excitatory motoneurones, the slow (SETi) and fast (FETi) extensor tibiae motoneurones, and by the common inhibitor motoneurone 1 (CI1). This simple type of innervation allows the complete description of the motoneuronal activity of the extensor muscle during changes in gain of the feedback system. For this muscle, it was found that most of the changes in gain in the inactive animal are based exclusively on changes in the activity of the SETi (see below), while FETi and CI1 remain inactive; therefore, the SETi was investigated in most detail.

The SETi motoneurone

In the inactive animal, the SETi motoneurone is spontaneously active. Its discharge frequency increases when the animal is disturbed, e.g. by tactile stimulation, and afterwards declines slowly to reach the pre-stimulus value (Fig. 2). Sinusoidal fCO stimulation causes an approximately sinusoidal modulation of SETi discharge over the stimulus cycle: the motoneurone is activated during elongation of the fCO and its discharge is reduced during relaxation (Figs 1, 2). Fig. 4 demonstrates the good correspondence between the phase histograms of sinusoidally modulated SETi discharge frequency and the simulated sinusoidal modulations of spike frequencies. Mean activity (mean) and amplitude of modulation (mod) of the SETi neurone discharge may vary over a wide range, depending both on the stimulus conditions and on internal parameters of the animal which are not under the control of the experimenter. In many experiments, the amplitude of modulation exceeded the mean activity. Under these conditions, the sinusoidally modulated instantaneous spike frequency took the form of a sine wave clipped at the 0 Hz line, i.e. during a certain phase of the fCO stimulus cycle,

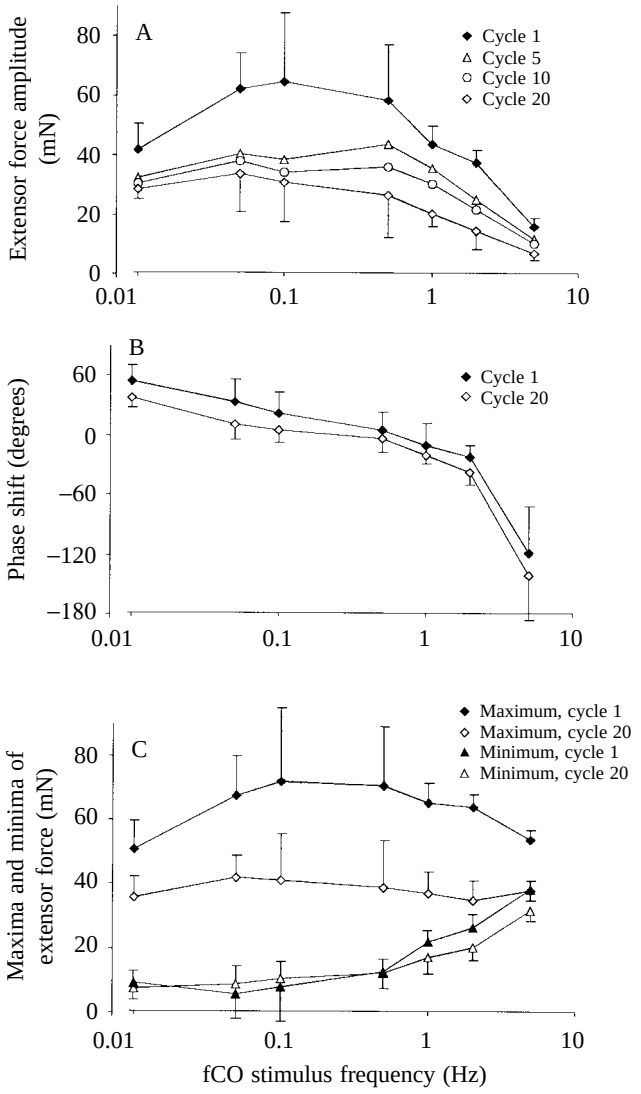

Fig. 3. Extensor muscle force during repetitive sinusoidal stimulation of the femoral chordotonal organ (fCO). Stimulus amplitude was 300 µm. Values are means for $N \geqslant 8$ stimulus trains from three animals; standard deviations are indicated for cycles 1 and 20; other standard deviations are not shown for clarity, but were similar. (A) Amplitude frequency–response curve for stimulus cycles 1, 5, 10 and 20. These curves show the band-pass characteristics of the system with an upper corner frequency of approximately 2 Hz. For all stimulus frequencies tested, a significant decrease in extensor force amplitude (paired *t*-test, $P<0.01$) occurred between the first and the twentieth cycle. (B) Phase shifts between maximum fCO elongation and maximum extensor muscle force for the first and twentieth stimulus cycles. During repetitive sinusoidal fCO stimulation, only minor phase shifts to smaller phase values occurred for all stimulus frequencies (see text). (C) Maxima and minima of extensor force. The decrease in force amplitude from the first to the twentieth cycle shown in A is caused by a significant decrease in the force maxima at all stimulus frequencies (paired *t*-test, $P<0.01$), whereas force minima remain relatively constant. A significant increase in the force minima with stimulus frequency (between 0.05 Hz and 5 Hz, $P<0.01$, *U*-test) occurs for cycles 1 and 20 as the muscle is no longer able to relax fully within the short cycle duration present at higher stimulus frequencies.

spike activity was inhibited. This could result from high amplitudes of modulation (caused by high fCO stimulus amplitudes or high gain values, e.g. Figs 1, 2) or from low values of mean activity (which could result from a decrease in gain, e.g. Fig. 4B).

Gain increases for small stimulus amplitudes

SETi discharge was analysed during repetitive sinusoidal fCO stimulation at a frequency of 0.5 Hz and with amplitudes of 0.05, 0.1, 0.3 and 0.5 mm, simulating tibial movements (FT angles) of 10°, 20°, 60° and 100° around a central position of 90°. Quantitative data from experiments on five animals are shown in Fig. 5. For each stimulus amplitude, at least 200 cycles from 10 stimulus trains (20 cycles each) were evaluated. Values for fCO stimulus amplitudes of 0.05 and 0.5 mm were compared using the *U*-test.

The mean values of the SETi mean activity (Fig. 5A, mean) show a weak, but not significant, increase with increasing stimulus amplitude ($P>0.1$). The mean vector length (Vl), which provides a measure of the distribution of the spikes of the SETi neurone within the stimulus cycle (see Materials and methods), increases ($0.1>P>0.05$) with increasing stimulus amplitude. The amplitude of modulation (mod, $P<0.01$) and the maximum activity (max, $P<0.01$) exhibit a significant increase with stimulus amplitude (Fig. 5A). At the smallest stimulus amplitude, 0.05 mm, the mean vector length was near 0.5 and therefore maximum activity was approximately twice mean activity. The increased vector length observed at higher stimulus amplitudes represents a sharper activity distribution. The spikes are therefore concentrated within a certain range of phase angles of the stimulus cycle and the discharge is inhibited during the rest of the cycle (e.g. Figs 1, 2, 4B). This explains the lack of a significant change in the mean activity (mean) because, during this inhibition, there is no spike frequency contribution to the mean activity (see Materials and methods). The computer simulation of the experimental spike distributions for the different stimulus amplitudes showed that the mean value ($mean_s$) remained constant, while the modulation (mod_s) increased with an increase in stimulus amplitude (see Materials and methods). This indicates that, during an increase of the fCO stimulus amplitude, the synaptic input to the motoneurone might show an increased modulation but no shift in the mean value of the membrane potential. The phase shift between maximum fCO elongation and maximum SETi discharge was approximately 54° at 0.05 mm stimulus amplitude and increased significantly ($P<0.05$) to approximately 70° at 0.3 or 0.5 mm stimulus amplitude (Fig. 5B).

A tenfold increase in stimulus amplitude caused no significant change in mean activity and an increase in amplitude of modulation of SETi discharge by a factor of only 1.9, while the maximum frequency increased by a factor of 1.5 (Fig. 5A). The small increases in these parameters, when compared with the tenfold increase in stimulus amplitude, describes a new non-linearity of the system. Small-amplitude fCO stimuli are relatively more effective in modulating the SETi discharge than are high-amplitude stimuli. They are

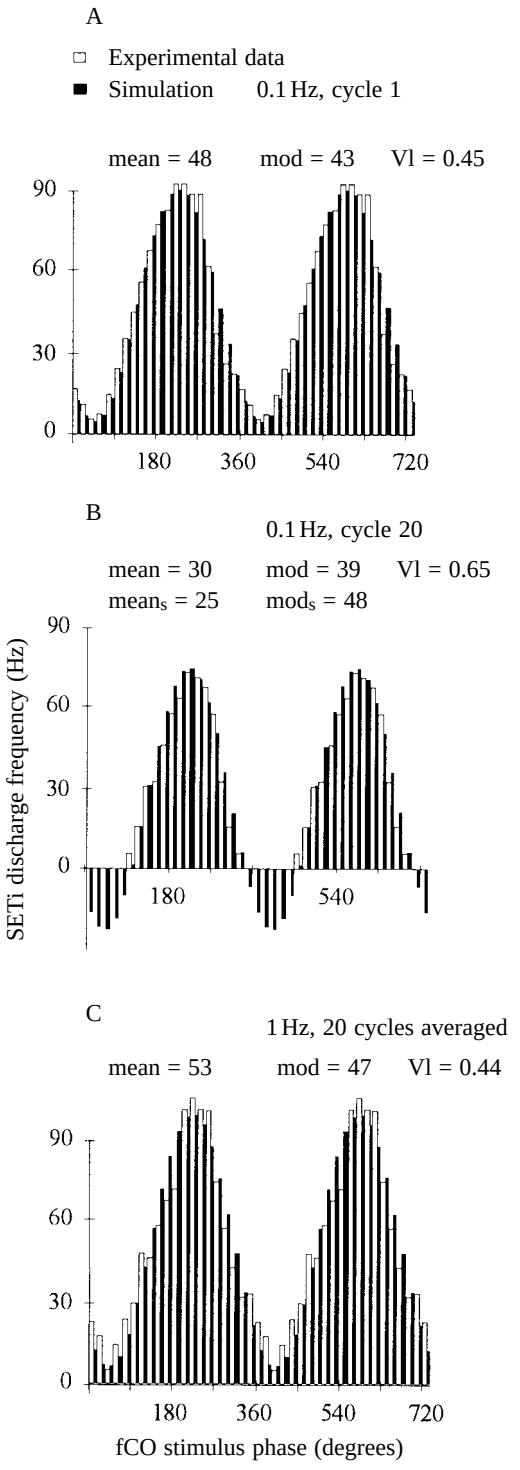

Fig. 4. Modulation of the activity of the slow extensor tibiae motoneurone (SETi) during sinusoidal stimulation of the femoral chordotonal organ (fCO), presented as phase histograms (bin width 36 °). Note the correspondence between the SETi discharge frequency from experimental data (open bars) and from simulations (filled bars). Stimulus cycles with high gain (first cycle, A) and low gain (twentieth cycle, B) from the same stimulus train (fCO stimulus frequency 0.1 Hz) are shown. The decrease in gain is accompanied by a decrease in mean activity (mean) and modulation amplitude (mod) and by an increase in the mean vector length (Vl). In B, the discharge is inhibited for phase angles between 0 ° and 90 °. Therefore, the circular statistics from the experimental data (mean, mod) differ from the simulated values ($mean_s$, mod_s) that describe the recorded spike distribution. The simulated values therefore better represent the input to the motoneurone (see Materials and methods and Fig. 13Cii). (C) Sinusoidal discharge modulation for an fCO frequency of 1 Hz (20 cycles averaged). For a better visual presentation of the sine wave, the data from the phase histogram are shown for two cycles.

therefore transmitted with a higher gain. Relative gain (Fig. 5A) was calculated from these data as the ratio of SETi modulation amplitude to fCO stimulus amplitude (set to 1 for 0.05 mm fCO amplitude). This non-linearity appears to be the neuronal origin of the similar stimulus amplitude *versus* gain curve of the whole FT feedback system and is an important property that preserves the stability of the system (Kittmann, 1991; see Discussion).

The decrease in SETi response with repetitive fCO stimulation was similar for all stimulus amplitudes: mean activity and maximum activity decreased from the first to the twentieth stimulus cycle. This indicates that the non-linearities described above were present both in the dishabituated (first cycle) and in the habituated (twentieth cycle) system.

Two mechanisms increase SETi modulation at high stimulus frequencies

The SETi discharge recorded during repetitive sinusoidal fCO stimulation was analysed at stimulus frequencies between 0.01 Hz and 10 Hz with a stimulus amplitude of 0.3 mm (60 ° FT angle). Experiments were carried out on five animals. For each frequency, at least 10 stimulus trains consisting of 50 cycles each were evaluated. Owing to the long duration of the experiment, the number of stimulus trains was reduced to six for the lowest stimulus frequency (0.01 Hz).

The mean value of the mean activity of the SETi neurone increased with increasing stimulus frequency (Fig. 6A). At frequencies between 0.01 and 2 Hz, the distribution of SETi spikes in the stimulus cycle, characterised by the mean vector length, did not change significantly (e.g. first cycle Vl=0.60–0.64, *U*-test, $P>0.1$; Fig. 6B). The significant increase in amplitude of modulation of SETi discharge (Fig. 6B) with increasing stimulus frequency between 0.01 and 2 Hz is therefore caused by the significant increase in mean activity ($P<0.05$). For the highest stimulus frequencies (5 and 10 Hz), there was a significant increase in the mean vector length (between 0.5 Hz and 5 or 10 Hz, first cycle, $P<0.05$, *U*-test) to values of up to 0.78. For these stimulus frequencies, SETi modulation is affected both by an increase in mean activity and, in addition, by a sharper distribution of spikes within the stimulus cycle (greater Vl). This is a neuronal feature not described previously which compensates for the low-pass characteristics of the muscle by producing an increased amplitude of SETi modulation at high fCO stimulus frequencies. The concentration of the SETi discharge within a narrow phase angle of the stimulus cycle that is described by

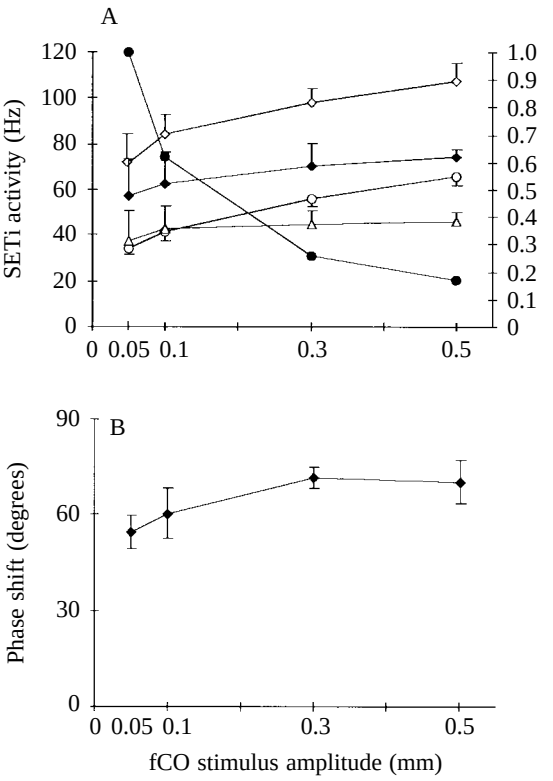

Fig. 5. SETi discharge variables during sinusoidal stimulation (0.5 Hz) of the femoral chordotonal organ (fCO) at different stimulus amplitudes. (A) The significant increases in the modulation amplitude (open circles) and maximum (open diamonds) of SETi discharge with stimulus amplitude are caused by a significantly sharper distribution (increased mean vector length Vl, filled diamonds) of the spikes within the stimulus cycle, while there is only a weak (not significant) increase in the mean activity (open triangles). The relative gain (filled circles), the ratio between SETi modulation and fCO stimulus amplitude (set to 1 for 0.05 mm fCO stimulus amplitude), decreases with increasing fCO stimulus amplitude. (B) The phase shift between maximum fCO elongation and maximum SETi discharge increases significantly with stimulus amplitude. Values are means ± S.D. ($N \geqslant 200$ cycles, 10 stimulus trains, five animals).

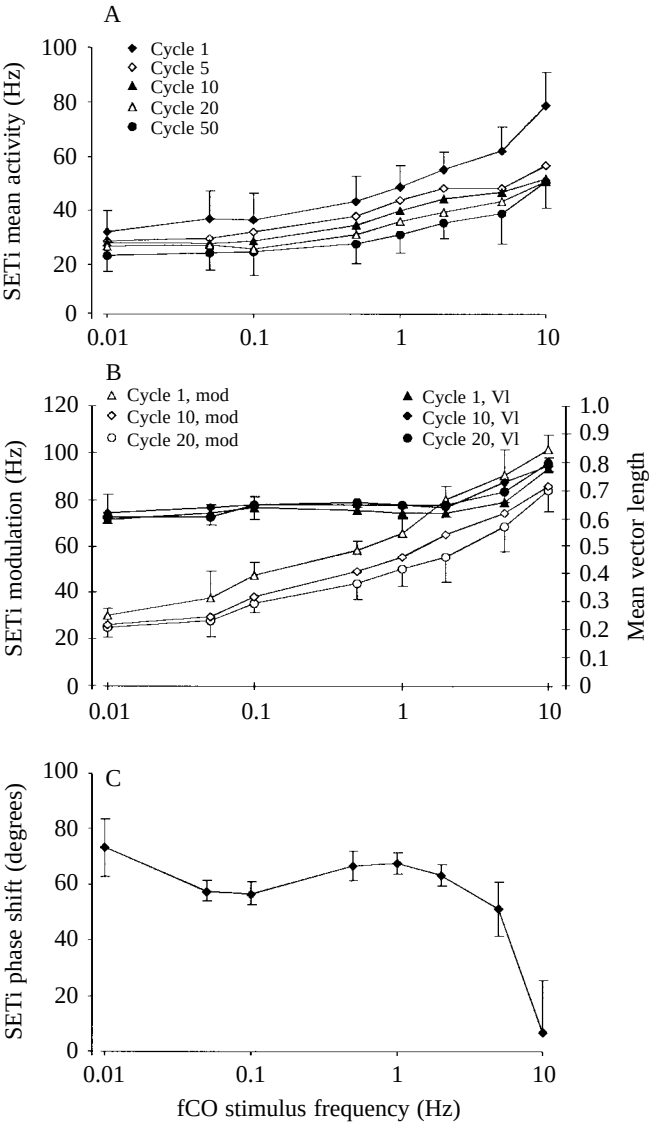

Fig. 6. SETi discharge variables *versus* stimulus frequency of the femoral chordotonal organ (fCO). (A) There is a significant increase in SETi mean activity with increasing fCO stimulus frequency. This causes an increase in SETi modulation amplitude (B), while the distribution of spikes within the stimulus cycle (the mean vector length, Vl) remains constant for stimulus frequencies from 0.01 to 2 Hz. For higher stimulus frequencies, the sharper distribution causes an additional increase in SETi modulation amplitude. During a stimulus train, the mean activity (A) and the modulation (B) significantly decrease from the first to the twentieth or fiftieth stimulus cycle. (C) Phase shift between maximum fCO elongation and maximum SETi discharge. fCO stimulus amplitude was 0.3 mm. Mean values from five animals (N>10). In A and B, standard deviation is indicated for the first and twentieth or fiftieth stimulus cycles only. Standard deviations for the other cycles were similar.

the increase in mean vector length is an essential requirement for increasing the upper corner frequency of the system; it enables the system to extend the duration of the relaxation phase of the muscle which limits the minimum force value and therefore the force amplitude (Fig. 3C).

The mean values of phase shift between maximum fCO elongation and maximum SETi discharge (Fig. 6C) were between 73 ° (at 0.01 Hz) and 57 ° (at 0.1 Hz) for fCO stimulus frequencies between 0.01 and 2 Hz. At 5 Hz and above, a significant decrease in phase values (between 0.5 Hz and 5 Hz or 10 Hz, P<0.01, U-test) was found. Nevertheless, even for stimulus frequencies up to 50 Hz (results not shown), SETi discharge remained phase-coupled.

Gain decreases during repetitive stimulation

At all stimulus frequencies, repetitive sinusoidal stimulation led to an exponential decrease in gain and in the modulation of the SETi discharge. Two alternative mechanisms were identified that reduced the modulation of the SETi discharge during repetitive fCO stimulation.

(i) The mean values of mean activity (Figs 6A, 7A) and of

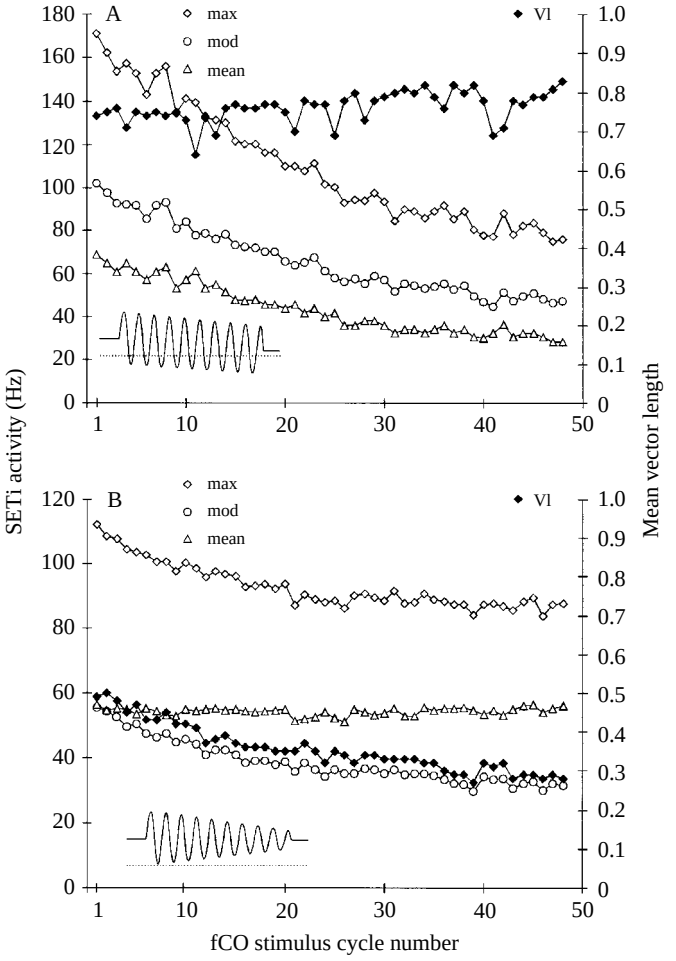

Fig. 7. Changes in SETi discharge variables during repetitive sinusoidal stimulation of the femoral chordotonal organ (fCO) caused by two different mechanisms. Both experiments show a decrease in maximum and modulation amplitude of SETi discharge during a stimulus train (50 cycles). This causes a reduced force amplitude in the extensor muscle (not shown). In A (fCO stimulus 2 Hz, 0.3 mm), this decrease is due to a reduced mean activity of the SETi neurone, while the weak increase in the mean vector length (Vl) indicates a slightly sharper distribution of spikes within the stimulus cycle. In contrast, in B (fCO stimulus 0.5 Hz, 0.3 mm), the mean activity remains constant. The decrease in motoneuronal activity is due to a changed spike distribution, described by a decrease in mean vector length (Vl). The insets demonstrate the mechanisms underlying the changes in 'neuronal gain' (see Discussion).

the amplitude of modulation (Figs 6B, 7A) decreased significantly for all stimulus frequencies (P<0.01, paired t-test) during repetitive stimulation. From the first stimulus cycle (100 %) to the twentieth stimulus cycle, the mean values of mean activity decreased to between 64 % (at 10 Hz) and 83 % (at 0.01 Hz). From the first to the twentieth stimulus cycle, the mean values of the amplitude of modulation of SETi discharge decreased significantly to between 84 % (at 0.01 Hz and 0.05 Hz) and 70 % (at 2 Hz). In most cases, the spike distribution (mean vector length) within the stimulus cycle remained constant or increased slightly during repetitive stimulation (Figs 6B, 7A). No significant changes in the phase relationship between SETi discharge and fCO stimulation were found during repetitive sinusoidal stimulation.

(ii) During some individual stimulus trains (approximately 5 % of the evaluated stimulus trains), an alternative mechanism for the decrease in gain during repetitive sinusoidal stimulation was observed. In contrast to the patterns described above, the decrease in gain in these cases was accompanied by a decrease in mean vector length, while the mean activity remained constant. This pattern also resulted in a reduction in maximum frequency and in the modulation of SETi discharge (Fig. 7B).

Induced and spontaneous changes in gain

The above data describe the motoneuronal representation of gain and its variation for three different stimulus conditions: a decrease in gain with increasing stimulus amplitude, a dependence of gain on stimulus frequency and a decrease in gain during repetitive sinusoidal stimulation. To obtain further information, changes in gain independent of these fCO stimulus parameters were evaluated (Figs 8–12). These changes in gain were recorded during continuous sinusoidal fCO stimulation. They possibly represent quantitative changes in the behavioural state of the inactive animal.

Three types of changes were observed. (i) Spontaneous changes in gain occurred in a few cases in the inactive animal. The FT movement amplitude and the gain increased or decreased within a few seconds (Fig. 8). (ii) In the inactive animal, the gain could usually be increased by weak tactile stimuli, e.g. delivered to the abdomen using a small paint brush (Figs 9, 10). (iii) In response to stronger repetitive tactile stimuli (and sometimes spontaneously), the animals became active, trying to move all their legs. Under daylight conditions, they returned to the inactive state within a period of several seconds to a minute. After such an episode, the gain had usually either decreased or increased (see Kittmann, 1991).

Changes in gain, measured as increases or decreases in the amplitude of the FT angle or extensor muscle force, were always accompanied by a parallel increase or decrease in the amplitude of modulation and the maximum frequency of SETi discharge (Figs 8, 9, 10). They were found to result from different parameter combinations of mean activity and spike distribution of the SETi discharge.

In Figs 8, 9 and 10, sequences in which spontaneous variations in gain occurred are shown for changes in FT angle amplitude and extensor muscle force. In Figs 9 and 10, an increase in gain induced by a tactile stimulus is also shown. The close correlations between the gain, measured as changes in FT angle amplitude (r=0.71, P<0.01) or extensor muscle force (r=0.91, P<0.01) and the amplitude of modulation of SETi discharge for these sequences is demonstrated graphically in Figs 11A and 12. The correlations between gain and mean activity (r=0.57, P<0.01) or the mean vector length (r=0.23, P<0.05) were much weaker. Similar SETi modulations, force amplitudes and FT amplitudes can result from different combinations of mean activity and mean vector length: high FT angle amplitudes and high SETi discharge

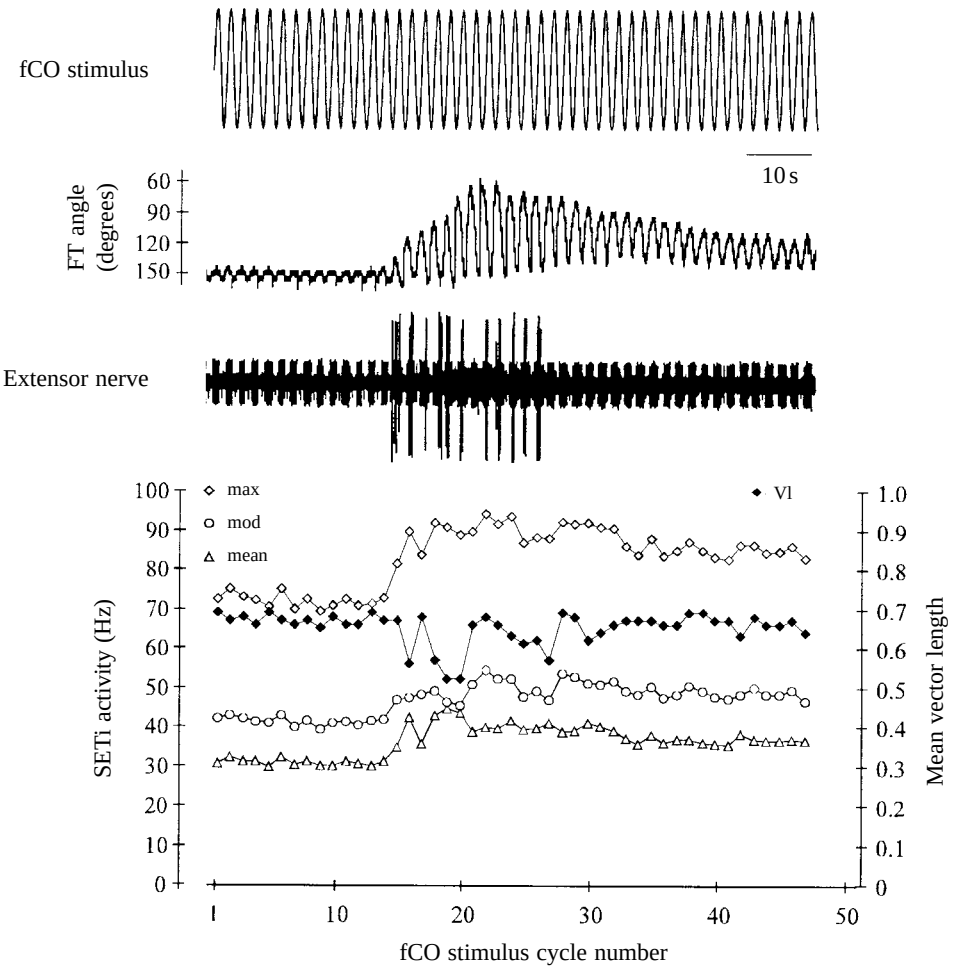

Fig. 8. Spontaneous increase in gain during repetitive sinusoidal stimulation of the femoral chordotonal organ (fCO). The increase in gain, measured as femor–tibia (FT) angle (middle trace), is accompanied by a FETi activation (large action potentials, lower trace) and an increase in the mean activity, modulation and maximum activity of the SETi neurone (graph). The distribution of spikes in the stimulus cycle (mean vector length, Vl) decreases or remains unchanged. fCO stimulus 0.5 Hz, 0.3 mm.

modulations result from high values of mean activity, from high values of mean vector length or from a combination of both these variables (Fig. 11B).

Strong increases in gain, in response to a tactile stimulus (Figs 9, 10), were always caused by a strong increase in the SETi mean activity while the mean vector length decreased, indicating a smoother distribution of spikes within the stimulus cycle. Nevertheless, this combination resulted in an increase in SETi modulation amplitude and gain.

Strong, sudden decreases in gain were normally based on a large decrease in the mean vector length (by 30–50 %, Fig. 9), while the mean activity often remained rather constant.

The FETi motoneurone

In the inactive stick insect, the FETi motoneurone is not spontaneously active. The animals showed strong individual differences in the responsiveness of the FETi neurone to tactile and fCO stimuli, irrespective of whether the tibia was free to move, whether it was connected to a force transducer or whether the flexor muscle was disconnected for measurement of the extensor force. In response to tactile stimuli, FETi spikes occurred in 90 % of the animals when active leg movements were elicited, while only 65 % of the inactive animals showed a FETi discharge. fCO stimuli only elicited FETi spikes in approximately 40 % of the animals (e.g. Figs 1, 8). Even within a single animal, the responsiveness of the FETi neurone to fCO stimuli could change during an experiment. Such changes often occurred following active leg movements or could be induced by tactile stimuli. Animals with a high feedback gain (measured as tibial movement) or a high neuronal gain for the SETi showed an increased probability of FETi discharge. fCO stimulation at stimulus frequencies below 0.1 Hz (0.3 mm stimulus amplitude) only rarely elicited spikes in the FETi neurone. For stimulus frequencies from 0.1 to 10 Hz, the probability that FETi spikes were elicited increased. FETi activity was modulated by the fCO stimulus. All spikes occurred within a narrow phase angle of the stimulus cycle, giving a mean vector length of greater than 0.85. The phase shift for maximum FETi activity was near the corresponding value for the SETi neurone. During repetitive fCO stimulation, FETi activity decreased to zero within a few cycles in most cases. Strong spontaneous increases in gain or those induced by a tactile stimulus were often accompanied by a FETi discharge for several stimulus cycles (Fig. 8).

In summary, the properties of FETi are in accordance with the results found for SETi. Excitation (mean activity) and modulation amplitude increase with fCO stimulus frequency and amplitude, and decrease with stimulus repetition. The

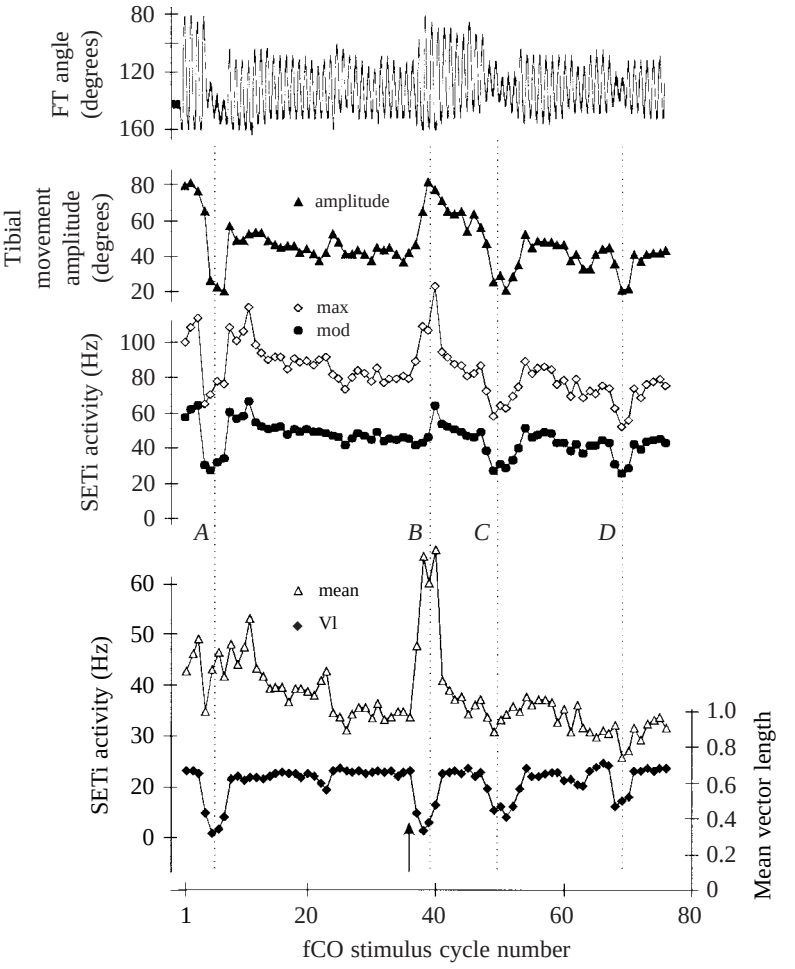

Fig. 9. Spontaneous and induced variation in gain. The close correlation between the modulation and the maximum frequency of SETi discharge and the femur–tibia (FT) movement amplitude is obvious. The prominent spontaneous decreases in gain (dotted vertical lines labelled *A*, *C* and *D*) are accompanied by a sudden decrease in SETi modulation amplitude and maximum activity. In this example, a smoother distribution of SETi spikes shown by the decrease in the mean vector length, Vl, is responsible for the reduced modulation amplitude and the weak apparent decrease in mean activity. The prominent increase in gain (dotted line labelled *B*) that was induced by a tactile stimulus (arrow) is characterised by a sudden increase in SETi maximum activity and modulation. The increase in SETi modulation is caused by a strong increase in mean activity while the mean vector length decreases. Traces show (from top to bottom): FT angle, tibial movement amplitude, SETi discharge frequency maximum, modulation amplitude and mean activity, and mean vector length.

excitation of both neurones is increased during spontaneous or induced increases in gain.

Discussion

The study contributes to the understanding of neuronal gain control in proprioceptive feedback systems. The quantitative data presented describe the neuronal parameters altered during gain control and allow differentiation between the neuronal mechanisms used in specific stimulus situations. These mechanisms can be correlated with, and probably underlie, specific changes in feedback gain that serve important functions in the regulation of the effectiveness and stability of the feedback response during adaptive behaviour. A model is proposed that interprets the observed changes in neuronal gain as the result of two pathways, one for stimulus-modulated information, the other carrying unmodulated information. The comparison of quantitative data on the FT angle, the extensor muscle force and the motoneuronal activity has revealed that new important non-linearities are present in the system. In particular, a neuronal mechanism that compensates for the low-pass characteristics of the muscle has been discovered.

Adaptivity and gain control in reflexes and feedback systems is a well-established and generalised phenomenon underlying adaptive behaviour. Several neuronal mechanisms have been demonstrated, and alternative architectures of the neuronal circuitries have been proposed that may form the basis of gain control (for reviews, see Prochazka, 1989; Bässler, 1993; Pearson, 1993; Burrows, 1994; Morton and Chiel, 1994). In proprioceptive feedback systems of insects, changes in the responsiveness of motoneurones (Bässler, 1976, 1986; Burrows, 1980; Weiland and Koch, 1987; Schmitz, 1993), interneurones (Siegler, 1981*b*; Laurent and Burrows, 1989; Büschges, 1990, 1995; Büschges and Schmitz, 1991; Büschges and Wolf, 1996) and sensory neurones (Ramirez *et al.* 1993; Burrows and Matheson, 1994) to proprioceptive stimuli have been demonstrated and are considered to be neuronal correlates of changes in gain. They can occur spontaneously, in response to elicited motor acts (e.g. Field and Burrows, 1982), in specific behavioural situations (e.g. Bässler, 1976, 1993; Cruse and Schmitz, 1983; Driesang and Büschges, 1996; Büschges and Wolf, 1996) or during specific experimental conditions such as during the application of neuromodulators (Büschges *et al.* 1993; Ramirez *et al.* 1993). Nevertheless, in many cases, it remains difficult to interpret the neuronal effects with respect to their contribution to and function in behaviour. There are only a limited number of studies that present the quantitative

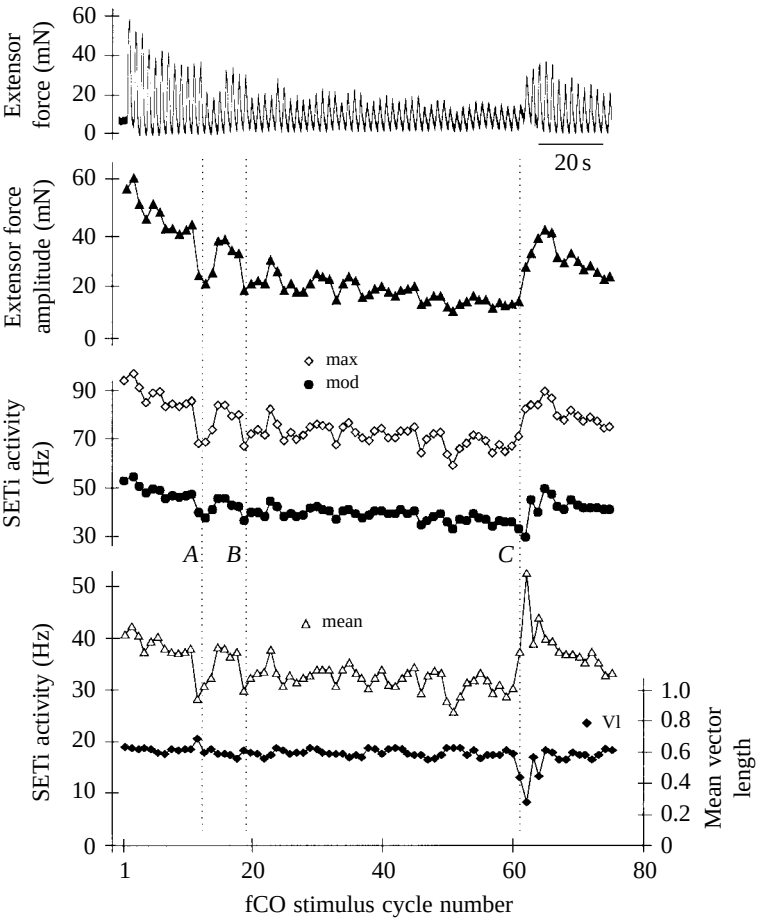

Fig. 10. Spontaneous and induced variations in gain for the extensor muscle force and the SETi discharge. Changes in extensor force amplitude (dotted lines labelled *A* and *B*) result from changes in mean activity, while the spike distribution (Vl) remains constant. The strong increase in gain (dotted line labelled *C*) induced by a tactile stimulus is caused by a strong increase in mean activity, although the mean vector length decreases. Traces show (from top to bottom): extensor force, extensor force amplitude, SETi discharge maximum, modulation amplitude and mean activity, and mean vector length.

data on the changes in responsiveness of neurones necessary to estimate their contribution and that can correlate the observed neuronal effects with the changes in the gain of the whole system under defined behavioural situations, a prerequisite for a functional interpretation (Cruse and Schmitz, 1983; Weiland and Koch, 1987; Bässler, 1993; Schmitz, 1993; Field and Coles, 1994; Büschges *et al.* 1993; Driesang and Büschges, 1993).

The present study takes advantage of the extensive knowledge gathered on the behavioural and neuronal function of the FT control loop in stick insects (e.g. Bässler, 1972*a*,*b*; Kittmann, 1991; Driesang and Büschges, 1993, 1996; Bässler and Nothof, 1994; for reviews, see Bässler, 1983*a*, 1993) and locusts (Burrows, 1974, 1987; Siegler, 1981*a*,*b*; Field and Burrows, 1982; Zill, 1985, 1987; Burrows *et al.* 1988; Burrows and Laurent, 1993; Field and Coles, 1994; Büschges and Wolf, 1995, 1996). This made it possible to investigate neuronal gain control in a system where its behavioural function is well understood. The gain control system of the femur–tibia control loop solves a problem present in many biological feedback systems. It adjusts the gain of this feedback loop to an optimal value, high enough for an effective feedback response, but limited to a critical upper value to prevent instability oscillations. A combination of several properties of this gain control system produces this function: an increase in gain following disturbing tactile stimuli, a decrease in gain with increasing stimulus amplitude, a decrease in gain with stimulus repetition and a dependency of gain on stimulus frequency (Kittmann, 1991).

Adaptive gain control in the inactive animal was measured for the whole system (as tibial movement, tibial torque or extensor muscle force) and, in parallel, for the motoneurones of the extensor muscle. All the important properties of the gain control system described above were found for these output functions. For the extensor muscle, gain is primarily determined by SETi discharge, while FETi is only phasically active for high fCO stimulus frequencies and amplitudes, and the CI1 neurone is scarcely active in the inactive animal. The close correlation between SETi discharge and the gain of the whole system during various types of changes in gain indicates that the SETi neurone plays an important role in gain control and/or that it reflects the properties of the other motoneurones (e.g. the flexor tibiae motoneurones) that determine the muscle forces and hence the movement amplitude of the tibia and the gain.

Neuronal gain

Gain in a technical sense is defined as the ratio of output to input signal amplitude. The FT control loop is one of the few biological feedback systems where absolute values of the gain

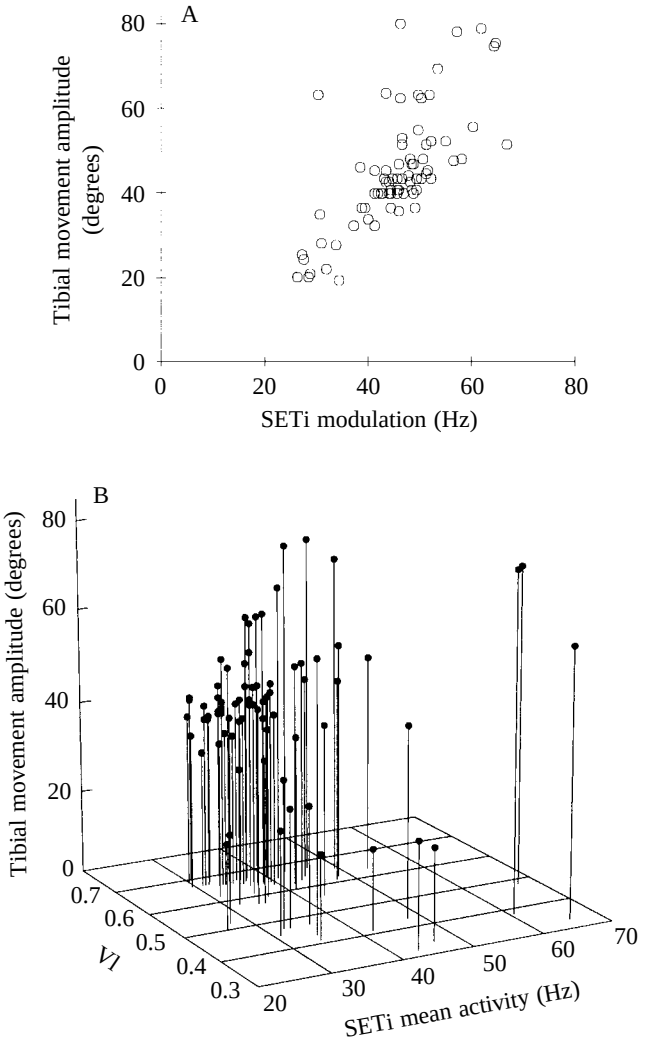

Fig. 11. Correlation between SETi discharge and gain. (A) There is a good correlation (r=0.71, P<0.01) between the gain of the whole system, measured as femur–tibia (FT) angle amplitude and SETi modulation amplitude for the sequence shown in Fig. 9. The correlations between FT angle amplitude and SETi mean activity (r=0.57, P<0.01) or the spike distribution (mean vector length, Vl) (r=0.23, P<0.05) were weaker. (B) Similar FT angle amplitudes (caused by high SETi modulations) can result from different combinations of the two parameters. High FT angle amplitudes result from high values of mean activity, from a sharper distribution of spikes (larger Vl) or from a combination of both parameters.

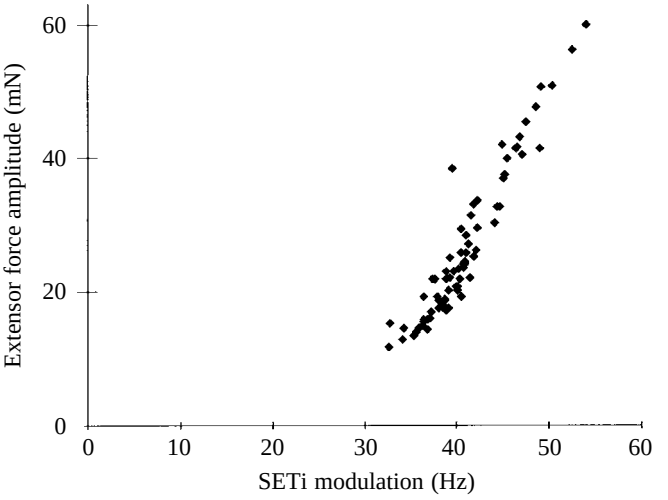

Fig. 12. Extensor muscle force amplitude *versus* SETi modulation amplitude. The close correlation (r=0.91, P<0.01) between the modulation amplitude of the SETi discharge and the extensor muscle force amplitude is demonstrated for the sequence shown in Fig. 10. During this sequence, the two other motoneurones in the extensor nerve, FETi and CI1, were not active. An increase from 30 to 60 Hz of SETi modulation leads to a fivefold increase in extensor force. This represents a strong non-linearity of the system, possibly based on facilitation properties of the extensor muscle.

can be calculated: the prerequisite that input and output amplitude can be converted to the same dimensions to calculate this ratio can be fulfilled (Bässler, 1972*b*, 1993). During investigations into the neuronal basis of gain control by measuring the transfer function between the sensory input and the different outputs (e.g. muscle force or neuronal activity), it is not possible to calculate the absolute value of gain as the input and output have different dimensions that cannot be compared. In this case, the ratio between output amplitude and input amplitude, now no longer dimensionless, can be used as a measure of gain. The comparison of changes in this ratio under stimulus conditions for which the gain of the whole system is known to change gives insights into the representation of gain in the measured output function. In the inactive stick insect, the force amplitude of the extensor muscle is often exclusively determined by the discharge of the SETi motoneurone. The amplitude of modulation of SETi discharge therefore reflects the ‘amplitude’ of neuronal activity and primarily determines the extensor muscle force amplitude and, thus, the tibial movement amplitude. The ratio of SETi modulation amplitude to the fCO stimulus amplitude can therefore be taken as a measurement of neuronal gain. The results demonstrate a good correlation between the neuronal gain and the gain of the whole system for several specific stimulus situations: the neuronal gain decreases with increasing stimulus amplitude and, during repetitive stimulation, it increases when the animal is disturbed and during spontaneous recovery during stimulus pauses. During spontaneous increases or decreases in gain, the neuronal gain also shows a similar pattern and time course (Fig. 9). The functions of all these changes in gain have been recognised previously as non-linearities that optimise and stabilise the feedback response of the system (Kittmann, 1991). Nevertheless, other parameters of the neuronal activity, the mean spike activity or spike distribution, might contribute to the muscle force amplitude and the gain. Thus, for example, similar SETi modulation amplitudes will cause different extensor muscle force amplitudes and tibial movement amplitudes when occurring at different values of SETi mean activity (Fig. 12).

Neuronal gain increases for small stimulus amplitudes

A new, important system characteristic is the prominent non-linearity between fCO stimulus amplitude and SETi modulation amplitude. Small fCO stimulus amplitudes are far more effective in modulating SETi discharge than are high amplitudes, which can be seen by comparing the ratio between the response and the stimulus. They are therefore transmitted with a higher gain. This non-linear gain *versus* stimulus amplitude function is likely to be the neuronal correlate of a similar function demonstrated for the whole system (Kittmann, 1991). This non-linearity is extremely important for gain control of the joint control loop. Low gain for high stimulus amplitudes enables the system to limit instability oscillations to a stable amplitude when gain increases to a critical value. Therefore, it is one of the main properties that preserve the stability of the gain control system. In contrast, a high gain for small stimulus amplitudes enables the system to detect and compensate even small deviations from the desired FT angle with a high accuracy, a general property demanded of feedback systems. This property is especially important for stick insects to produce catalepsy, a behaviour that supports twig mimesis (Bässler, 1972*a*, 1983*a*; Bässler and Foth, 1982). Even small fCO stimulus amplitudes corresponding to a 10° FT angle cause a spike distribution of SETi discharge with a mean vector length of approximately 0.5, resulting in minimum spike frequencies near zero and maximum frequencies of twice the mean frequency. This means that, even for small fCO stimuli, a spike distribution is produced for which co-contraction of the antagonistic muscles is minimal or prevented.

Velocity-sensitivity as a mechanism to produce a non-linear stimulus amplitude versus *gain curve*

The increase in gain with a decrease in stimulus amplitude (or *vice versa*) shown for sine-wave stimuli is in accordance with results from experiments using ramp-wise stimulation of the fCO in stick insects. For ramp functions, extremely low stimulus velocities induce strong resistance reflexes to produce catalepsy (Bässler, 1972*a*). This has been shown for the tibial movement (Bässler and Foth, 1982), for the SETi discharge and for the depolarisation of the FETi and SETi (Bässler, 1983*a*,*b*).

In the locust, motoneurones which have different properties with respect to stimulus velocity have been described, some with increased sensitivity (Field and Burrows, 1982), others with decreased sensitivity (Büschges and Wolf, 1995). Although, in these studies, the gain has not been calculated with respect to the stimulus velocity, the data indicate that the gain of these systems increases with decreasing stimulus velocity.

Slow fCO stimulus speeds occur in slow ramp functions and in low-amplitude sine-wave functions, and the high gain under these conditions may therefore be based on the same mechanism. It is conceivable that the non-linear velocity-sensitivity of the system, which gives a possible increase in gain with decreasing stimulus velocity, is a mechanism that helps to produce a non-linear gain *versus* stimulus amplitude curve. The indirect presynaptic inhibitory interactions of fCO sensilla found in the locust (Burrows and Laurent, 1993; Burrows and Matheson, 1994) could also form the basis for this non-linearity: they were considered to form an automatic gain control system that could reduce the gain for high stimulus amplitudes.

Non-linearities between FT amplitude, extensor muscle force and motoneuronal modulation during changes in gain

Quantitative measurements of the three output functions, the FT angle, the extensor muscle force and the motoneuronal activity, during changes in gain document new non-linearities of the feedback system. For tibial movements, extreme values of 50-fold changes in gain were measured. During repetitive sinusoidal stimulation with a constant stimulus amplitude and at different stimulus frequencies, the gain decreased to between 5 and 30 % of the initial value (Kittmann, 1991). For the extensor force amplitude, extreme 6.4-fold changes were found and the average decreases in force amplitude (to 39–68 % of the initial values, Fig. 3) and SETi modulation amplitude (to 70–93 % of the initial values, Fig. 5) during repetitive stimulation were smaller. Large changes in gain measured as changes in tibial movement amplitude in the open-loop feedback system correspond to smaller changes in amplitude of extensor muscle force and even smaller changes in motoneuronal modulation amplitude. In other words, small changes in the modulation amplitude of motoneuronal discharge result in larger changes in muscle force amplitude (see also Fig. 12) and even larger changes in gain, measured from the tibial movement amplitude. The results using different stimulus amplitudes support these findings: for tibial movement, the gain increases by a factor of 2.3–3.8 when the stimulus amplitude is reduced by a factor of 10 (Kittmann, 1991), while the motoneuronal gain calculated as SETi modulation amplitude *versus* fCO stimulus amplitude increases by a factor of less than 5 (Fig. 5). When calculating the changes in output amplitude that correspond to this reduction in stimulus amplitude, the results also show that minor changes in motoneuronal modulation amplitude (by a factor of 2) result in over-proportional changes in movement amplitudes (by a factor of 2.6–4.4).

It seem unlikely that these non-linearities can be explained by the contribution of the flexor muscle (which is also involved in gain control): during changes in gain measured as tibial movement, the mean value of the FT angle can remain constant, increase or decrease (Figs 8, 9; Kittmann, 1991). This suggests that both muscles are involved in gain control and that the changes in movement amplitude can be produced by symmetrical or asymmetrical changes in the force amplitudes of the antagonistic muscles. Nevertheless, to interpret changes in the neuronal output in terms of the gain of the feedback system, direct measurement of the non-linearities between motoneuronal discharge and muscle force will be necessary. In particular, facilitation properties, such as those described for motoneuronal synapses of slow motoneurones in other insects (Hoyle, 1965), may also be present for the SETi and may

contribute to the non-linearity between motoneuronal discharge, muscle force and gain (Fig. 12).

Two mechanisms increase the neuronal gain to compensate for the low-pass characteristics of the muscle

At the level of tibial movement, the FT feedback system is a bandpass filter. Its lower corner frequency is extremely low and its upper corner frequency is approximately 2 Hz (Bässler, 1972*b*, 1993, 1996). The shape of the amplitude–frequency curve depends on the gain of the system (Kittmann, 1991). Similar characteristics are found for the extensor force (Fig. 3; see also Storrer and Cruse, 1977). For SETi discharge, in contrast, the modulation amplitude (neuronal gain) increases with increasing stimulus frequency. This property, which has also been demonstrated for the coxotrochanteral feedback system (Schmitz, 1986), will increase the force amplitude of the extensor muscle and therefore will partially compensate the decrease in force amplitude that occurs at high fCO stimulus frequencies. It therefore increases the speed and improves the dynamics of the feedback system.

Two neuronal mechanisms are involved in this compensation. For the whole range of stimulus frequencies, an increase in mean activity is responsible for the increased modulation amplitude (see also Bässler, 1983*b*; Kittmann and Schmitz, 1992; Bässler and Stein, 1996). In addition, a sharper distribution of spikes within the stimulus cycle has been identified as a new mechanism by which the upper corner frequency of the system is increased. It concentrates the neuronal activation within a narrow phase angle of the stimulus cycle and therefore increases the period available for the relaxation of the muscle (which primarily determines its low-pass characteristics) (Fig. 6).

For fCO stimulus frequencies above 2 Hz, the phase shift between SETi modulation amplitude and fCO stimulus increases strongly. The main factors that control this phase shift are the latency due to the conduction times in the pathways from the fCO to the motoneurone and the dynamics of the circuitry. For example, a latency of 17 ms would explain the increase in the phase shift by approximately 60 ° that occurs in response to an increase in the fCO stimulus frequency from 1 to 10 Hz (Fig. 6); but how realistic is this value? Latencies of approximately 8 ms have been measured between step functions to the fCO and the responses of the extensor motoneurones recorded in the neuropile (Driesang and Büschges, 1996). With an additional delay of approximately 4 ms from the neuropile of the motoneurones to the middle of the femur length (10 mm), where the extracellular recordings were obtained, this gives an estimated latency of approximately 12 ms. The remaining difference of approximately 5 ms might be explained by the dynamics of the circuit, which may exhibit a faster response to step functions with high acceleration than to sine-wave functions.

Mechanisms of neuronal gain control

The modulation amplitude of SETi discharge results from two independent parameters, the mean spike activity and the distribution of spikes over the stimulus cycle (see Materials and methods). Therefore, the same SETi modulation and thus the same neuronal gain can be produced by different combinations of these parameters. Changes in gain elicited under specific stimulus conditions are based on characteristic changes in these parameters of SETi discharge. They therefore underlie different neuronal mechanisms. The mechanisms of gain control described below are demonstrated in Fig. 13 for results from computer simulations.

(i) The distribution of spikes within the stimulus cycle can change, while the mean activity remains constant (Fig. 13, mechanism i), i.e. when the stimulus amplitude is altered. It is a mechanism sometimes found during spontaneous or induced changes, especially for decreases in gain. It also occurs (although more rarely) during repetitive sinusoidal stimulation (Fig. 7B). For analogue signals in technical systems such as operational amplifiers, this is the principle that normally describes changes in gain.

The modulation amplitude of SETi discharge may also be changed by two other parameter combinations that are both based on a change in the mean activity of the motoneurone.

(ii) The modulation amplitude of SETi discharge can be altered by changes in mean activity because of the presence of a spike threshold (Fig. 13, mechanism ii). Changes in mean activity will change SETi modulation amplitude and gain if the mean activity does not fall below the value of the modulation amplitude. However, when the mean activity decreases below this value, discharge is inhibited for part of the stimulus cycle. As the spike activity cannot have negative values, this causes a decrease in SETi modulation amplitude: maximum SETi discharge decreases but the minimum remains near zero, even though only the mean value but not the amplitude of the synaptic input to the motoneurone, modulated by the fCO stimulus, has changed. This mechanism would imply that mean activity and modulation amplitude are two parameters that can be controlled independently by the nervous system. The additive effects of the mean activity input and the modulation input would define the actual SETi spike discharge and distribution.

(iii) Changes in SETi modulation amplitude could be caused by changes in mean activity while the distribution of spikes over the stimulus cycle (characterised by the mean vector length) remains constant (Fig. 13, mechanism iii). The presence of this mechanism implies that mean activity and spike distribution are input parameters that can be independently controlled by the nervous system, while the modulation amplitude of the discharge frequency results from a multiplication of the effects of these two inputs.

Using the present results, mechanisms ii and iii are difficult to distinguish, as they produce similar results for spike distributions with a mean vector length above 0.5, when the mean activity falls below the value of modulation amplitude. An important question to answer in future experiments is which of the parameters (mean activity, modulation amplitude and spike distribution) can be independently controlled by the nervous system? In particular, are modulated and unmodulated

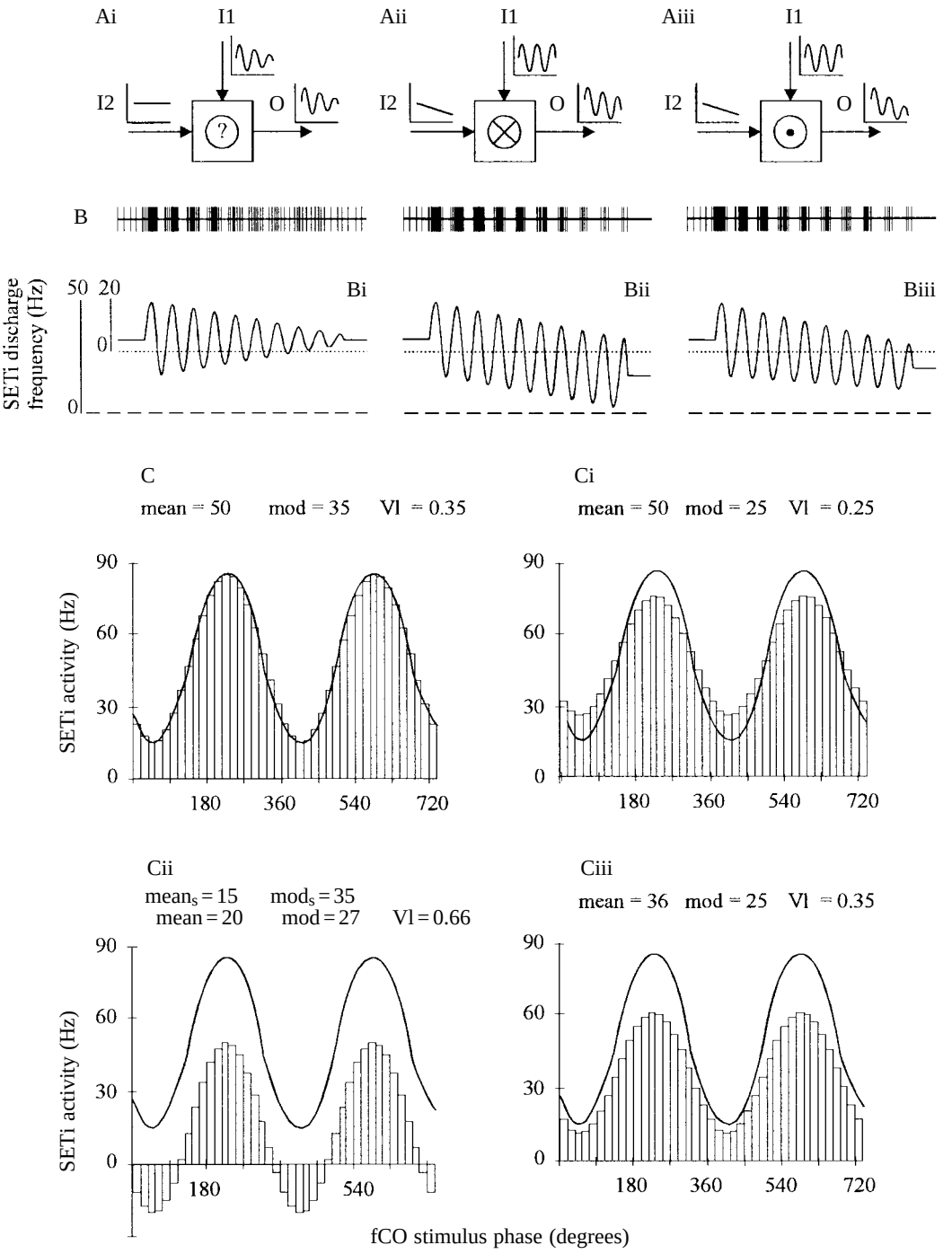

Fig. 13. Mechanisms of gain control. (A) Schematic drawing of the three mechanisms of gain control. The output (O) of the neurone is determined by the two inputs, I1 and I2. I1 represents the stimulus-modulated information from the fCO and I2 determines the mean activity. In Ai, only the value of I1 changes (it is reduced): SETi modulation and the mean vector length therefore decrease, while the mean activity remains constant. Aii and Aiii show alternative mechanisms. In Aii, the output results from the addition of the two inputs I1 and I2. A decrease in mean activity (I2) leads to a decrease in SETi modulation when the neurone is inhibited for part of the cycle because of the spike threshold. In Aiii, the output results from multiplication of the two inputs. A decrease in mean activity (I2) then automatically leads to a decrease in SETi modulation while the distribution remains constant. (B) Sine-wave functions showing modulation of the SETi discharge (instantaneous frequency) during a continuous decrease in gain simulated for the three mechanisms shown in A. The scale 0–50 Hz on the left indicates the case when the modulation amplitude is smaller than the mean activity. The neurone is active during the whole stimulus cycle as the minimum discharge frequency does not reach the spike threshold (dashed line). The scale 0–20 Hz demonstrates the case when the modulation amplitude exceeds the mean activity. The neurone's discharge is inhibited during part of the stimulus cycle as the neurone is hyperpolarized below the spike threshold (dotted line). Schematic drawings of extracellular recordings are given. (C) The decrease in SETi modulation amplitude from 35 Hz (upper left; indicated by the sine function) to 25 Hz is simulated for the three postulated mechanisms shown in A (i, ii, iii) and is plotted as phase histograms. In Ci, the modulation (input I1) decreases, while the mean activity (input I2) remains constant (Fig. 7B). This leads to a smoother distribution of spikes over the stimulus cycle (decrease in Vl). In Cii, the modulating input (I1, mod_s 35 Hz) remains constant but the input for the mean activity decreases (I2, $mean_s$ 15 Hz). Therefore, the discharge is modulated between 0 and 50 Hz, and the neurone is inhibited for part of the stimulus cycle. The modulation amplitude is 25 Hz. The modulation of the discharge no longer represents a pure sine function as it is clipped by the spike threshold. Therefore, the values of the mean activity (mean, 20 Hz), modulation (mod, 27 Hz) and the spike distribution (Vl, 0.66) calculated using circular statistics differ from the values used for the simulation, which represent the synaptic input to the neurone ($mean_s$, mod_s; see Materials and methods). In Ciii, the output results from multiplication of the two inputs for modulation (I1) and mean activity (I2); a decrease in mean activity (I2) therefore automatically leads to a decreased modulation of the SETi discharge while the distribution (Vl) remains constant.

information combined by a neuronal addition process (e.g. mechanism ii) or a multiplication process (e.g. mechanism iii)? This could be answered in future studies using small stimulus amplitudes in which the mean vector length does not exceed 0.5 and the two mechanisms can clearly be distinguished. Behaviourally important changes in gain are based on one of the mechanisms that alter the mean activity, e.g. most of the spontaneous or touch-induced increases in gain, the increase in neuronal gain with increasing fCO stimulus frequency and the decrease in gain during instability oscillations or repetitive fCO stimulation.

Model of neuronal gain control

From the present results, it is possible to describe the output of the SETi neurone during sinusoidal fCO stimulation as a function of two separate inputs I1 and I2 (Fig. 13A). Depending on the stimulus conditions, the two inputs can be independent of each other or have specific couplings. The output (O) of the SETi neurone (Fig. 13A), especially the modulation amplitude, results from a combination of these two inputs.

(1) The first input (I1) represents the pathway that supplies stimulus-modulated information from the fCO, directly and/or *via* the interneurones to the motoneurones. Its strength increases with fCO stimulus amplitude.

(2) The second input (I2) supplies tonic information that defines the spontaneous activity of the SETi neurone, as long as no modulated fCO stimulus is present. During sinusoidal fCO stimulation, it does not supply modulated information, but its tonic value increases with increasing fCO stimulus frequency. Its value decreases during repetitive fCO stimulation and is almost independent of the stimulus amplitude.

Spontaneous or touch-induced changes in gain are heterogeneous and can be caused by changes in one or both inputs. Increases in gain are often caused by an increase in the second input (I2), while I1 remains constant. Spontaneous decreases in gain are normally due to a decrease in I1. However, in some cases, alternative parameter combinations can be observed.

Neuronal realisation of gain control

Although the model described above might be useful as a tool to distinguish different neuronal mechanisms of gain control, we should not expect to find distinct structures within the real neuronal circuit that represent the two postulated inputs or their point of convergence. Within the neuronal circuitry of the FT feedback system, neuronal mechanisms that could underlie gain control have been demonstrated at almost all neuronal levels. Non-linearities between the mechanical stimulus, fCO movement and the sensory output represented by approximately 80 sensory neurones in the ventral cord of the fCO (Kittmann and Schmitz, 1992) have been demonstrated in stick insects (Hofmann *et al.* 1985) and in the locust (Matheson, 1990; Field and Coles, 1994). They could form the basis of the dependency of gain on fCO stimulus parameters such as amplitude, frequency or velocity. However, the presynaptic gain control mechanism that acts on the fCO afferents may also contribute to these characteristics (Burrows and Laurent, 1993; Burrows and Matheson, 1994; Wolf and Burrows, 1995). The decrease in gain found during repetitive fCO stimulation and the subsequent spontaneous recovery might derive partially from sensory adaptation. Habituation and dishabituation (e.g. by tactile stimuli) demand an interaction between interneuronal pathways that receive convergent information from proprioceptive and exteroceptive sense organs (Burrows, 1989; Laurent and Burrows, 1989). These characteristics have been shown for many of the nonspiking interneurones of the FT feedback system (Schmitz *et al.* 1991; Büschges *et al.* 1994; Kittmann *et al.* 1996). They might change the balance of the antagonistic pathways in the parallel, distributed circuitry that has been demonstrated to underlie the feedback system (Büschges and Schmitz, 1991; Büschges, 1990, 1995; Sauer *et al.* 1996). Furthermore, results indicate that a tonic, unmodulated activation or inhibition of the extensor or flexor motoneurones could act as an effective mechanism of gain control. Neuromodulators such as octopamine act on the sensory cells (Ramirez *et al.* 1993) and on central neurones of the circuit and might also contribute to gain control, especially with regard to the behavioural state (inactive, active) of the stick insect (Büschges *et al.* 1993). To determine where the structures involved in gain control are located and what mechanisms they use, further intracellular investigations are necessary. Such studies will have to establish the relevance of the mechanisms described above under stimulus conditions in which behaviourally relevant changes in gain occur (locust: Büschges and Wolf, 1996). In particular, the idea that there might be two different types of neuronal pathway, both important in gain control, will have to be considered in further experiments: pathways that carry fCO stimulus-modulated information and change their strength during gain control (mechanism i, Fig. 13) and pathways that do not carry fCO stimulus-modulated information but receive a tonic activation or inhibition during changes in gain (mechanisms ii and iii, Fig. 13).

I am grateful to two anonymous referees for their helpful comments and suggestions. In addition, I thank S. Knotz, Dr J. Schmitz and Dr H. Wolf for critically reading the manuscript.

References

BÄSSLER, D., BÜSCHGES, A., MEDITZ. S. AND BÄSSLER, U. (1996). Correlation between muscle structure and filter characteristics of the muscle–joint system in three orthopteran insect species. *J. exp. Biol.* **199**, 2169–2183.

BÄSSLER, U. (1972*a*). Der Regelkreis des Kniesehnenreflexes bei der Stabheuschrecke *Carausius morosus*: Reaktionen auf passive Bewegungen der Tibia. *Biol. Cybernetics* **12**, 8–20.

BÄSSLER, U. (1972*b*). Der Regelkreis des Kniesehnenreflexes bei der Stabheuschrecke *Carausius morosus*: Übergangsfunktion und Frequenzgang. *Biol. Cybernetics* **12**, 32–50.

BÄSSLER, U. (1976). Reversal of a reflex of a single motoneuron in the stick insect *Carausius morosus*. *Biol. Cybernetics* **24**, 47–49.

BÄSSLER, U. (1983*a*). *Neural Basis of Elementary Behavior in Stick Insects. Studies of Brain Function*. Berlin: Springer.

BÄSSLER, U. (1983*b*). The neural basis of catalepsy in the stick insect *Cuniculina impigra*. III. Characteristics of the extensor motor neurons *Biol. Cybernetics* **46**, 159–165.

BÄSSLER, U. (1986). Afferent control of walking movements in the stick insect *Cuniculina impigra*. II. Reflex reversal and the release of the swing phase in the restrained foreleg. *J. comp. Physiol.* A **158**, 351–362.

BÄSSLER, U. (1993). The femur–tibia control system of stick insects – a model system for the study of the neural basis of joint control. *Brain Res. Rev.* **18**, 207–226.

BÄSSLER, U. AND FOTH, E. (1982). The neural basis of catalepsy in the stick insect *Cuniculina impigra*. I. Catalepsy as a characteristics of the femur–tibia control system. *Biol. Cybernetics* **45**, 101–105.

BÄSSLER, U. AND NOTHOF, U. (1994). Gain control in a proprioceptive feedback loop as a prerequisite for working close to instability. *J. comp. Physiol.* A **175**, 23–33.

BÄSSLER, U. AND STEIN, W. (1996). Contribution of structure and innervation pattern of the stick insect extensor tibiae muscle to the filter characteristics of the muscle–joint system. *J. exp. Biol.* **199**, 2185–2198.

BATSCHELET, E. (1981). *Circular Statistics in Biology*. London: Academic Press.

BLOEM, B. R., BECKLEY, D. J., REMLE, M. P., ROOS, R. A. C. AND VAN DIJK, J. G. (1995). Postural reflexes in Parkinson's disease during 'resist' and 'yield' tasks. *J. neurol. Sci.* **129**, 109–119.

BURROWS, M. (1974). The organization of inputs to motorneurons of the locust metathoracic leg. *Phil. Trans. R. Soc. Lond. B* **269**, 49–94.

BURROWS, M. (1980). The control of sets of motoneurones by local interneurones in the locust. *J. Physiol., Lond.* **298**, 213–233.

BURROWS, M. (1987). Parallel processing of proprioceptive signals by spiking local interneurons and motor neurons in the locust. *J. Neurosci.* **7**, 1064–1080.

BURROWS, M. (1989). Processing of mechanosensory signals in local reflex pathways of the locust. *J. exp. Biol.* **146**, 209–227.

BURROWS, M. (1992). Local circuits for the control of leg movements in an insect. *Trends Neurosci.* **15**, 226–232.

BURROWS, M. (1994). The influence of mechanosensory signals on the control of leg movements in an insect. In *Neural Basis of Behavioural Adaptations* (ed. K. Schildberger and N. Elsner), pp.145–165. New York: Gustav Fischer Verlag.

BURROWS, M. AND LAURENT, G. J. (1989). Reflex circuits and the control of movement. In *The Computing Neuron* (ed. R. Durbin, C. Miall and G. Mitchison), pp. 244–261. New York: Adison-Wesley.

BURROWS, M. AND LAURENT, G. J. (1993). Synaptic potentials in the central terminals of locust proprioceptive afferents generated by other afferents from the same sense organ. *J. Neurosci.* **13**, 808–819.

BURROWS, M., LAURENT, G. J. AND FIELD, L. H. (1988). Proprioceptive inputs to nonspiking local interneurons contribute to local reflexes of a locust hindleg. *J. Neurosci.* **8**, 3085–3093.

BURROWS, M. AND MATHESON, T. (1994). A presynaptic gain control mechanism among sensory neurons of a locust leg proprioceptor. *J. Neurosci.* **14**, 272–282.

BÜSCHGES, A. (1990). Nonspiking pathways in a joint-control loop of the stick insect *Carausius morosus*. *J. exp. Biol.* **151**, 133–160.

BÜSCHGES, A. (1995). Plasticity of neuronal networks that control posture and movement of leg joints in insects. *Verh. dt. zool. Ges.* **88**, 139–151.

BÜSCHGES, A., KITTMANN, R. AND RAMIREZ, J.-M. (1993). Octopamine effects mimic state-dependent changes in a proprioceptive feedback system. *J. Neurobiol.* **24**, 598–610.

BÜSCHGES, A., KITTMANN, R. AND SCHMITZ, J. (1994). Identified nonspiking interneurons in leg reflexes and during walking in the stick insect. *J. comp. Physiol.* A **174**, 685–700.

BÜSCHGES, A. AND SCHMITZ, J. (1991). Nonspiking pathways antagonize the resistance reflex in the thoraco-coxal joint of stick insects. *J. Neurobiol.* **22**, 224–237.

BÜSCHGES, A. AND WOLF, H. (1995). Nonspiking local interneurons in insect leg motor control. I. Common layout and species-specific response properties of femur–tibia joint control pathways in stick insect and locust. *J. Neurophysiol.* **73**, 1843–1860.

BÜSCHGES, A. AND WOLF, H. (1996). Gain changes in sensorimotor pathways of the locust leg. *J. exp. Biol.* **199**, 2437–2445.

CRUSE, H. AND SCHMITZ, J. (1983). The control system of the femur–tibia joint in the standing leg of a walking stick insect *Carausius morosus*. *J. exp. Biol.* **102**, 175–185.

CRUSE, H. AND STORRER, J. (1977). Open loop analysis of a feedback mechanism controlling the leg position in the stick insect *Carausius morosus*: Comparison between experiment and simulation. *Biol. Cybernetics* **25**, 143–153.

DAVIS, L. L. AND O'LEARY, D. P. (1993). Autorotation tests of the horizontal vestibulo-ocular reflex in Meniere's disease. *Otolaryngol. Head Neck Surgery* **109**, 399–412.

DICAPRIO, R. A. AND CLARAC, F. (1981). Reversal of a walking leg reflex elicited by a muscle receptor. *J. exp. Biol.* **90**, 197–203.

DRIESANG, R. B. AND BÜSCHGES, A. (1993). The neural basis of catalepsy in the stick insect. IV. Properties of nonspiking interneurons. *J. comp. Physiol.* **173**, 445–454.

DRIESANG, R. B. AND BÜSCHGES, A. (1996). Physiological changes in central neuronal pathways contributing to the generation of a reflex reversal. *J. comp. Physiol.* A (in press).

EL MANIRA, A., CATTEART, D. AND CLARAC, F. (1990). Reflex reversal and presynaptic control of sensory afferents in Crustacea. *Eur. J. Neurosci.* (Suppl.) **3**, 183.

EL MANIRA, A., CATTEART, D. AND CLARAC, F. (1991). Monosynaptic connections mediate resistance reflex in crayfish (*Procambarus clarkii*) walking legs. *J. comp. Physiol.* **168**, 337–349.

FIELD, L. H. AND BURROWS, M. (1982). Reflex effects of the femoral chordotonal organ upon leg motor neurones of the locust. *J. exp. Biol.* **101**, 265–285.

FIELD, L. H. AND COLES, M. L. (1994). The position-dependent nature of postural resistance reflexes in the locust. *J. exp. Biol.* **188**, 65–88.

HEUKAMP, U. (1983). Die Rolle von Mechanorezeptoren im Flugsystem der Wanderheuschrecke (*Locusta migratoria* L.): Übertragungseigenschaften und Analyse der Wirkung auf die Flugmotorik. Dissertation, Universität Köln.

HOFMANN, T., KOCH, U. T. AND BÄSSLER, U. (1985). Physiology of the femoral chordotonal organ in the stick insect, *Cuniculina impigra*. *J. exp. Biol.* **114**, 225–237.

HOYLE, G. (1965). Neural control of skeletal muscle. In *The Physiology of Insecta II* (ed. M. Rockstein), pp. 407–449. London: Academic Press Inc.

JELLEMA, T. AND HEITLER, W. J. (1996). Peripheral control of the gain of a central synaptic connection between antagonistic motor neurones in the locust. *J. exp. Biol.* **199**, 613–625.

KIRSCHFELD, K. (1991). An optomotor control system with automatic

compensation for contrast and texture. *Proc. R. Soc. Lond. B* **246**, 261–268.

KIRSCHFELD, K. (1992). Oscillations in the insect brain: Do they correspond to the cortical γ-waves of vertebrates? *Proc. natn. Acad. Sci. U.S.A.* **89**, 4764–4768.

KITTMANN, R. (1984). Quantitative Analyse von Verstärkungsänderungen eines Gelenkstellungsregelkreises. Dissertation, Universität Kaiserslautern.

KITTMANN, R. (1991). Gain control in the femur–tibia feedback system of the stick insect. *J. exp. Biol.* **157**, 503–522.

KITTMANN, R. AND SCHMITZ, J. (1992). Functional specialization of the scolopidia of the femoral chordotonal organ in stick insects. *J. exp. Biol.* **173**, 91–108.

KITTMANN R., SCHMITZ, J. AND BÜSCHGES A. (1996). Premotor interneurons in the generation of adaptive leg reflexes and voluntary movements in the stick insect. *J. Neurobiol.* **31**, 512–532.

LAURENT, G. AND BURROWS, M. (1989). Intersegmental interneurons can control the gain of reflexes in adjacent segments of the locust by their action on nonspiking local interneurons. *J. Neurosci.* **9**, 3030–3039.

MATHESON, T. (1990). Responses and locations of neurones in the locust methathoracic femoral chordotonal organ. *J. comp. Physiol.* **166**, 915–927.

MORTON, D. W. AND CHIEL, H. J. (1994). Neural architectures for adaptive behavior. *Trends Neurosci.* **17**, 413–419.

PEARSON, K. G. (1993). Common principles of motor control in vertebrates and invertebrates. *A. Rev. Neurosci.* **16**, 265–297.

PROCHAZKA, A. (1989). Sensorimotor gain control: a basic strategy of motor systems? *Prog. Neurobiol.* **33**, 281–307.

RAMIREZ J.-M., BÜSCHGES A. AND KITTMANN, R. (1993). Octopaminergic modulation of the femoral chordotonal organ in the stick insect. *J. comp. Physiol.* **173**, 209–219.

SAUER A. E., DRIESANG, R. B., BÜSCHGES, A. AND BÄSSLER, U. (1996). Information processing in the femur–tibia control loop of stick insects. I. The response characteristics of two nonspiking interneurons result from parallel excitatory and inhibitory inputs. *J. comp. Physiol.* A (in press).

SCHMITZ, J. (1985). Control of leg joints in stick insect: Differences in the reflex properties between the standing and the walking states. In *Insect Locomotion* (ed. M. Gewecke and G. Wendler), pp. 27–32. Berlin: Paul Parey.

SCHMITZ, J. (1986). The depressor trochanteris motoneurones and their role in the coxo-trochanteral feedback loop in the stick insect *Carausius morosus*. *Biol. Cybernetics* **55**, 25–34.

SCHMITZ, J. (1993). Load compensation reactions in the proximal leg joints of stick insects during standing and walking. *J. exp. Biol.* **183**, 15–33.

SCHMITZ, J., BÜSCHGES, A. AND KITTMANN, R. (1991). Intracellular recordings from nonspiking interneurons in a tethered walking insect. *J. Neurobiol.* **22**, 907–921.

SIEGLER, M. (1981*a*). Posture and history of movement determine membrane potential and synaptic events in nonspiking interneurons and motor neurons of the locust *J. Neurophysiol*. **46**, 296–309.

SIEGLER, M. (1981*b*). Postural changes alter synaptic interactions between nonspiking interneurons and motoneurons of the locust. *J. Neurophysiol.* **46**, 310–323.

SKORUPSKI, P., VESCOVI, P. J. AND BUSH, B. M. H. (1994). Integration of positive and negative feedback loops in a crayfish muscle. *J. exp. Biol.* **187**, 305–313.

STORRER, J. AND CRUSE, H. (1977). Systemanalytische Untersuchungen eines aufgeschnittenen Regelkreises, der die Beinstellung der Stabheuschrecke *Carausius morosus* kontrolliert: Kraftmessungen an den Antagonisten Flexor und Extensor Tibiae. *Biol. Cybernetics* **25**, 131–142.

WATERSTON, J. A., BARNES, G. R. AND GREALY, M. A. (1992). A quantitative study of eye and head movements during smooth pursuit in patients with cerebellar disease. *Brain* **115**, 1343–1358.

WEILAND, G. AND KOCH, U. T. (1987). Sensory feedback during active movements of stick insects. *J. exp. Biol.* **133**, 137–156.

WENDLER, G. (1964). Laufen und Stehen der Stabheuschrecke *Carausius morosus*: Sinnesborstenfelder in den Beingelenken als Glieder von Regelkreisen. *Z. vergl. Physiol.* **48**, 198–250.

WOLF, H. AND BURROWS, M. (1995). Proprioceptive neurons of a locust leg receive presynaptic inhibition during walking. *J. Neurosci.* **15**, 5623–5636.

ZILL, S. N. (1985). Plasticity and proprioception in insects. II. Modes of reflex action of the locust metathoracic femoral chordotonal organ. *J. exp. Biol.* **116**, 463–480.

ZILL, S. N. (1987). Selective mechanical stimulation of an identified proprioceptor in freely moving locusts: role of resistance reflexes in active posture. *Brain Res.* **417**, 195–198.